

Distribution Agreement

In presenting this thesis as a partial fulfillment of the requirements for a degree from Emory University, I hereby grant to Emory University and its agents the non-exclusive license to archive, make accessible, and display my thesis in whole or in part in all forms of media, now or hereafter now, including display on the World Wide Web. I understand that I may select some access restrictions as part of the online submission of this thesis. I retain all ownership rights to the copyright of the thesis. I also retain the right to use in future works (such as articles or books) all or part of this thesis.

Patricia Lin

March 18, 2019

In Situ Kinetic Studies on Rhodium (II) Carboxylate Catalysts with Cyclopropanation Reactions

by

Patricia Lin

Dr. Huw M. L. Davies
Adviser

Department of Chemistry

Dr. Huw M. L. Davies
Adviser

Dr. Nathan Jui
Committee Member

Dr. Paul Bhasin
Committee Member

2019

In Situ Kinetic Studies on Rhodium (II) Carboxylate Catalysts with Cyclopropanation Reactions

By

Patricia Lin

Dr. Huw M. L. Davies

Adviser

An abstract of
a thesis submitted to the Faculty of Emory College of Arts and Sciences
of Emory University in partial fulfillment
of the requirements of the degree of
Bachelor of Sciences with Honors

Department of Chemistry

2019

Abstract

In Situ Kinetic Studies on Rhodium (II) Carboxylate Catalysts with Cyclopropanation Reactions

By Patricia Lin

A systematic kinetics study was done via ReactIR™ on dirhodium catalysts with the cyclopropanation reaction to further understand the catalytic cycle, as well as the effect of the catalysts' ligands on the performance of the catalyst. Using the RPKA study, the rhodium (II) triarylcyclopropane carboxylate catalyst was found to be robust, as the catalytic activity is maintained during the course of the reaction. The rhodium (II) catalysts with different ligands exhibit different reactivities, some catalyzing the reaction faster than others; however, all of the catalysts tested were able to achieve at least 40,000 turnover numbers (TON). This study gives a better understanding of the factors that affect catalyst activity and stability under high TON conditions, and results from this study can help with the design of ligands that will lead to more efficient and practical rhodium (II) catalysts. It was also found that dimethylcarbonate (DMC) can be used as a greener alternative for solvent compared to dichloromethane (DCM), and not only does it give higher enantioselectivity, it allows for the use of lower catalyst loadings at higher temperatures.

In Situ Kinetic Studies on Rhodium (II) Carboxylate Catalysts with Cyclopropanation Reactions

By

Patricia Lin

Dr. Huw M. L. Davies

Adviser

A thesis submitted to the Faculty of Emory College of Arts and Sciences
of Emory University in partial fulfillment
of the requirements of the degree of
Bachelor of Sciences with Honors

Department of Chemistry

2019

Acknowledgements

I would like to thank my primary investigator, Dr. Huw Davies, for mentoring me and supporting my career in chemistry. I'm grateful to have had the opportunity to conduct research in his lab. He has given me the tools necessary to be successful in graduate school and I am lucky to have had such a great undergraduate research experience.

I would like to thank the other members of my thesis committee, Dr. Nathan Jui and Dr. Paul Bhasin. Dr. Jui has been a great professor and advisor to me in my undergraduate career, and I appreciate everything he has taught me and done for me as an advisor. Dr. Bhasin has been a wonderful professor/orchestra director of mine, and has been nothing but enthusiastic and supportive of my career in chemistry. I appreciate both of these professors for sitting on my committee.

I would like to thank Dr. Sidney Wilkerson-Hill for getting me started when I first joined the Davies group. He was extremely patient and helpful in teaching me laboratory techniques and critical thinking skills.

I would like to thank Bo Wei for working with me on this project for this past year. She has been a great partner in this project, and I wish her the best in her remaining years in graduate school and in the future.

Finally, I would like to thank everyone in the Davies group for providing me with guidance and support, and a great learning environment.

Table of Contents

| | |
|--|----|
| 1) Introduction | 1 |
| 1.1) Rhodium (II) Catalysts and Background | 1 |
| 1.2) Cyclopropanation Reaction and Carbenes | 2 |
| 1.3) High Turnover Numbers with Rhodium (II) Catalysts | 4 |
| 1.4) Reaction Progress Kinetic Analysis (RPKA) | 4 |
| 2) Results and Discussion | 5 |
| 2.1) Initial Studies with Triarylcyclopropane Carboxylate Catalysts | 5 |
| 2.2) Molecular Sieves as Drying Agent | 10 |
| 2.3) A Greener, Safer Solvent | 17 |
| 2.4) Discussion | 27 |
| 3) Conclusions | 29 |
| 4) Experimental | 30 |
| 4.1) General Remarks | 30 |
| 4.2) General Procedure for Synthesis of Diazo Compounds | 30 |
| 4.3) General Procedure of ReactIR™ Set-up and Cyclopropanation Reactions | 31 |
| 4.4) General Procedure for ReactIR™ Data Analysis | 33 |
| 4.5) Analysis of Cyclopropane Products | 34 |
| 4.6) HPLC Traces | 35 |
| References | 47 |

Figures and Tables

| | |
|-----------------|----|
| Figure 1 | 1 |
| Figure 2 | 3 |
| Figure 3 | 3 |
| Figure 4 | 5 |
| Figure 5 | 6 |
| Figure 6 | 6 |
| Figure 7 | 7 |
| Figure 8 | 7 |
| Figure 9 | 8 |
| Table 1 | 8 |
| Figure 10 | 9 |
| Table 2 | 10 |
| Figure 11 | 10 |
| Table 3 | 11 |
| Figure 12 | 12 |
| Table 4 | 12 |
| Table 5 | 13 |
| Figure 13 | 14 |
| Table 6 | 14 |
| Table 7 | 15 |
| Figure 14 | 15 |
| Table 8 | 16 |

| | |
|-----------------|----|
| Table 9 | 16 |
| Figure 15 | 17 |
| Table 10 | 17 |
| Table 11 | 18 |
| Figure 16 | 19 |
| Table 12 | 19 |
| Figure 17 | 20 |
| Table 13 | 20 |
| Figure 18 | 21 |
| Table 14 | 21 |
| Figure 19 | 22 |
| Table 15 | 23 |
| Figure 20 | 23 |
| Table 16 | 24 |
| Figure 21 | 24 |
| Table 17 | 25 |
| Figure 22 | 25 |
| Table 18 | 26 |
| Figure 23 | 26 |
| Table 19 | 27 |
| Figure 24 | 32 |
| Figure 25 | 33 |

1) Introduction

1.1) Rhodium (II) Catalysts

Rhodium catalysts are useful in many asymmetric transformations because of its high reactivity and selectivity; however, the rarity of the metal poses a cost issue, making it expensive to run reactions that utilize rhodium as catalysts. In order to avoid the high cost of using rhodium-based catalysts in asymmetric transformations, chemists can use other transition metals, such as copper or zinc, which are much cheaper than rhodium, or find ways to reuse rhodium catalysts from reaction to reaction. However, other transition-metal catalysts have not been found to be as effective with respect to reactivity and selectivity as rhodium, and recycled rhodium catalysts have been found to be less reactive and selective than fresh catalysts.

Due to its ability to transfer cheap starting material into chiral product, rhodium catalysts have been found to be useful in the pharmaceutical industries as well as natural product syntheses in research groups. The Huw Davies group have synthesized various dirhodium (II) catalysts with different ligands, such as the proline¹, phthalamido, and the triarylcyclopropane carboxylate² (Figure 1).

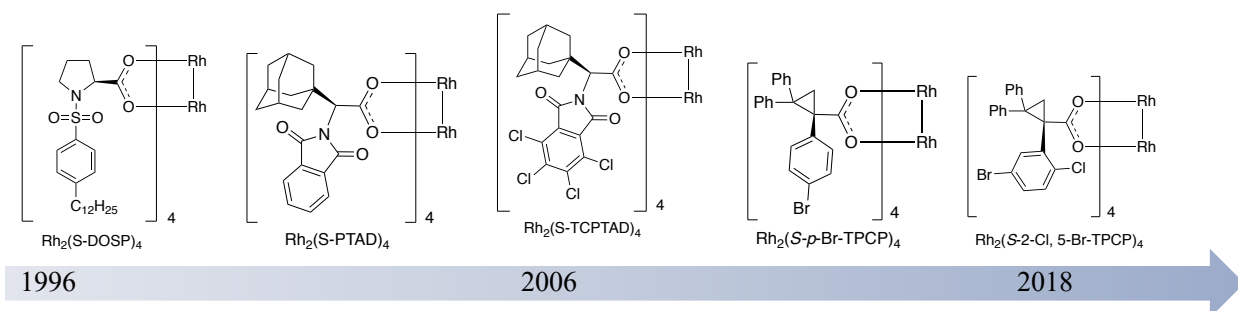


Figure 1: Davies Group Rhodium (II) Catalysts Timeline

Each of the catalysts synthesized by the Davies group have an overall paddlewheel framework. The proline-based ligands make up the first-generation catalysts, with the $\text{Rh}_2(\text{S-DOSP})_4$ (dodecyl sulfonyl proline) catalyst exhibiting high enantio- and diastereoselectivity with

cyclopropanation reactions¹. Since the $\text{Rh}_2(\text{S-DOSP})_4$ catalyst, many catalysts, including $\text{Rh}_2(\text{S-PTAD})_4$ which has been found to catalyze the cyclopropanation reaction with very high enantioselectivity, have been developed for C-H functionalization. Each of these have different reactivities and specialties, where one catalyst selectively inserts into C-H bonds at the primary position³, another performing C-H amination selectively⁴, and so on. The third generation of dirhodium (II) catalysts developed in the Davies group, the triarylcyclopropane carboxylate catalysts, has been found to not only selectively insert into primary C-H bonds, but also catalyze the cyclopropanation reaction of trichloroethyl aryldiazoacetates with an olefin at high levels of enantioinduction⁵.

1.2) Cyclopropanation Reaction and Carbenes

The cyclopropanation reaction creates three-membered rings, which are ubiquitous in natural products⁶ and pharmaceutical products⁷. Because of the ubiquity of these fragments, new practical methods must be developed to synthesize cyclopropanated products effectively and selectively. Rhodium-catalyzed cyclopropanation reactions of diazocarbonyls have been found to be a powerful method to synthesize cyclopropanes; however, these cyclopropanation reactions have low selectivity. It has been found that when using a chiral rhodium catalyst, specifically $\text{Rh}_2(\text{S-DOSP})_4$, a highly enantioselective cyclopropanation reaction is possible, where the complexation of the diazoester to the rhodium, leading to the loss of N_2 , gives the rhodium carbenoid, and the chirality of the catalyst contributes to the high levels of enantioselectivity⁸.

The cyclopropanation reaction with styrene occurs via the donation of electron density from the electron-rich alkene group of styrene to the carbene carbon, creating a bond between the primary carbon on styrene and the carbene. The creation of the bond between the primary carbon of styrene and the carbene forms a partial positive charge on the secondary carbon of styrene,

which is stabilized by the ester group from the diazo compound. The stereochemistry observed in the cyclopropane product comes from the electron density from the carbene bond moving towards the secondary carbon of styrene, resulting in a trans relationship between the aryl group of styrene and the ester group from the diazo compound¹.

The known mechanism of the catalytic cycle of the rhodium (II) catalyst in cyclopropanation reaction is shown below (Figure 2)⁹.

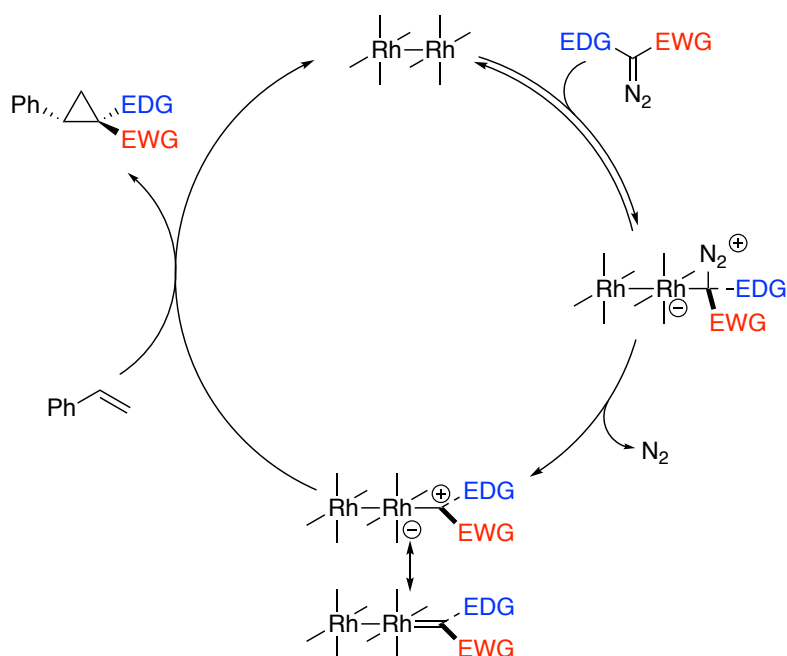


Figure 2: Catalytic Cycle of the Rhodium-catalyzed Cyclopropanation Reaction

For the cyclopropanation reaction using rhodium (II) catalysts, it has been found that the donor-acceptor carbenes¹⁰, although least reactive of the three kinds of carbenes, are the most selective, especially for the cyclopropanation reaction (Figure 3).

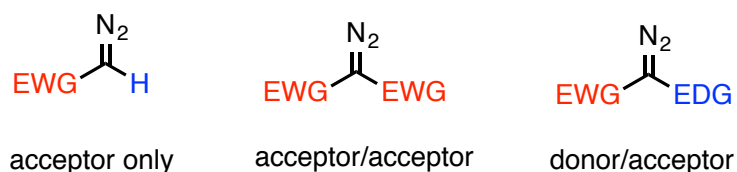


Figure 3: Classes of Carbene

1.3) High Turnover Numbers with Rhodium (II) Catalysts

Because of the high cost of rhodium, due to it being a precious and rare metal, achieving high turnover numbers (TON) in rhodium-catalyzed reactions is important to alleviate the cost of conducting reactions with rhodium, where TON can be calculated by Equation 1.

$$TONs = \frac{\text{moles of product produced}}{\text{moles of catalyst used}} \quad (1)$$

It was found that the $\text{Rh}_2(\text{S-DOSP})_4$ is capable of TONs up to 900,000, using a catalyst loading as low as 0.00005 mol% in solvent-free conditions¹¹. However, the level of enantioselectivity and the time of the reaction (69% ee in 144 hours)¹¹, as well as the exothermic nature of the reaction, makes this result unfavorable, especially in large-scale reactions. The necessity of high TON conditions that maintain a high level of enantioselectivity is apparent here after these studies to achieve high TON cyclopropanation reactions with rhodium (II) catalysts failed to maintain the enantioselectivity observed at higher catalyst loadings.

1.4) Reaction Progress Kinetic Analysis (RPKA)

Developed by Dr. Donna Blackmond, the Reaction Progress Kinetic Analysis (RPKA)¹² is a methodology to analyze a catalytic reaction and develop a mechanistic model by using continuous, *in situ* measurements and a minimal number of experiments. By manipulating data obtained from the ReactIRTM, and combining the data with the RPKA methods, a more detailed understanding of the catalytic activity of dirhodium (II) catalysts in cyclopropanation can be achieved. These studies include the “same excess” experiment to probe the robustness of the catalyst, and whether or not the product plays a role in the catalytic activity of the catalyst during the reaction, and “different excess” experiments to understand the concentration dependence of various reagents used in the system, both of which will be explained in detail in the latter sections.

2) Results and Discussion

Since the first dirhodium (II) catalyst, $\text{Rh}_2(\text{S-DOSP})_4$ was introduced, many other catalysts, including catalysts with the phthalamido-based ligands and the triarylcyclopropane carboxylate ligands, have been synthesized and have made significant impacts on dirhodium catalyst-based chemistry. Although previous kinetics studies have been done with the DOSP catalyst¹³, a more systematic study was completed with the newer, triarylcyclopropane carboxylate catalysts.

2.1) Initial studies with Triarylcyclopropane Carboxylate Catalysts

2.1.1) Relative Reactivities

In order to understand the relative reactivities of the different catalysts from the 3rd-generation triarylcyclopropane carboxylate catalysts, five different catalysts were screened at a 0.01 mol% catalyst loading in dichloromethane (Figure 4).

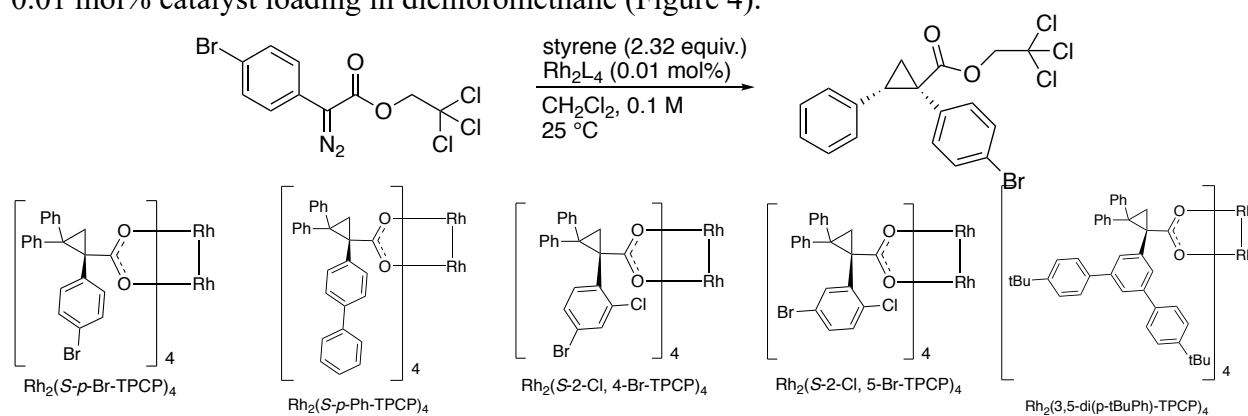


Figure 4: Cyclopropanation Reaction with Triarylcyclopropane Carboxylate Catalysts

The reaction was monitored by the Mettler Toledo ReactIR™ 45m instrument, which can follow the change in concentration of the desired compound *in situ* throughout the reaction. In this study, the diazo compound's decomposition was followed by the IR peak of diazo at 2103 cm^{-1} (Figure 5).

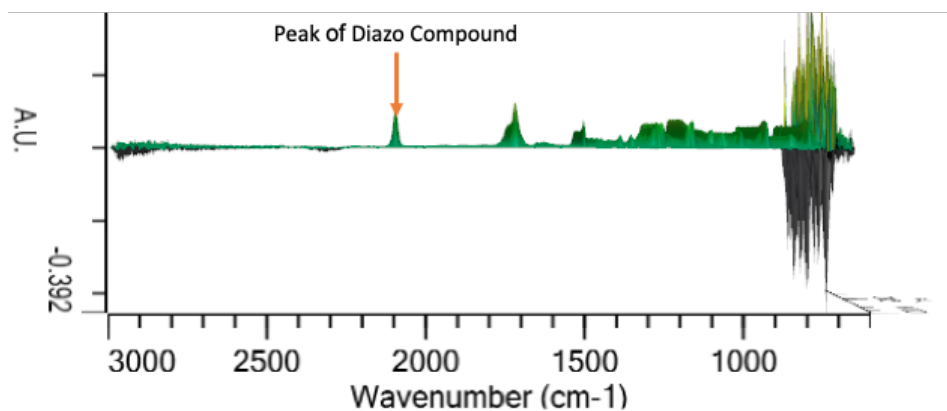


Figure 5: Diazo IR Peak on the ReactIR™ Software

The diazo peak (2103 cm^{-1}), the styrene peak (917 cm^{-1}), and the cyclopropane product peak (1738 cm^{-1}), were followed during the course of a reaction, and the relative concentrations of each of the three compounds were plotted against time (Figure 6).

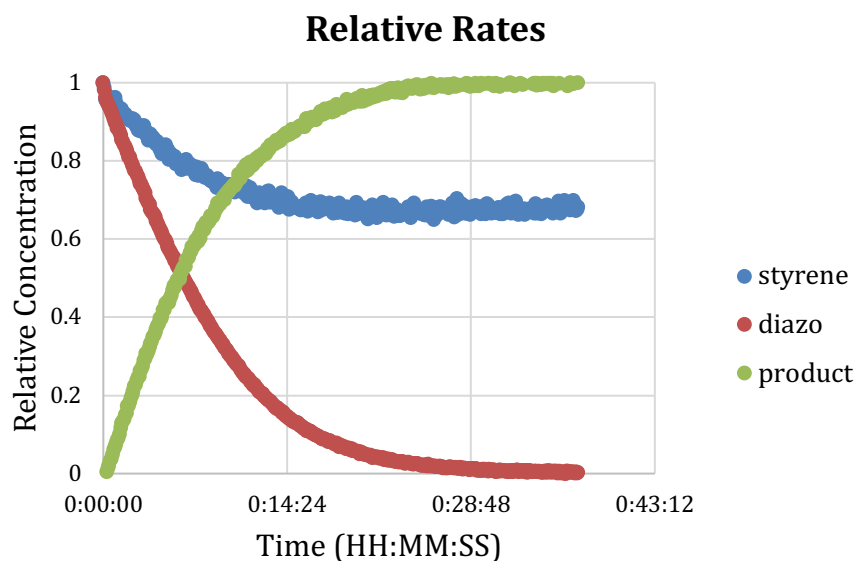


Figure 6: Relative Rates of Diazo, Styrene, and Cyclopropane Product

When the cyclopropane product concentration was subtracted from 1 and plotted against the diazo decomposition curve, there was a good overlap of the two curves (Figure 7).

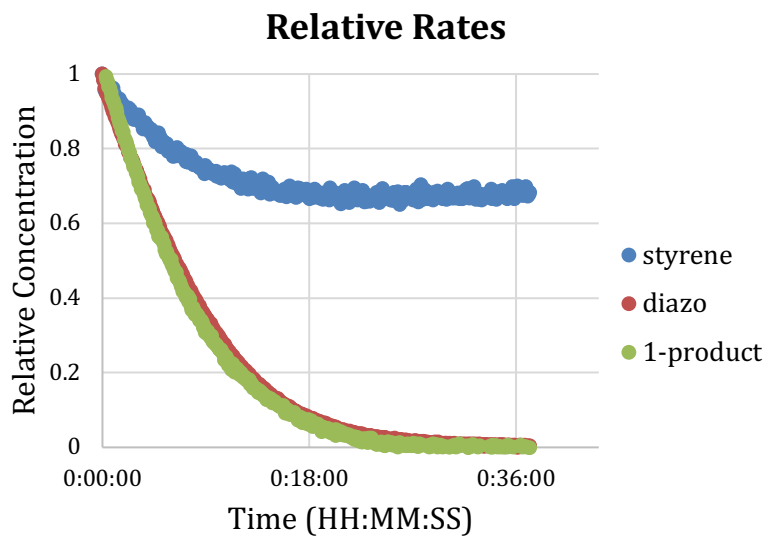


Figure 7: Relative Rates with 1-[product] Plotted Against Diazo Decomposition

This overlap between the diazo decomposition curve and the (1-[product]_{rel}) curve shows that it is possible to follow the diazo decomposition curve for this experiment because the diazo compound is being converted to only the desired cyclopropane product, with no byproducts being synthesized (Figure 8).

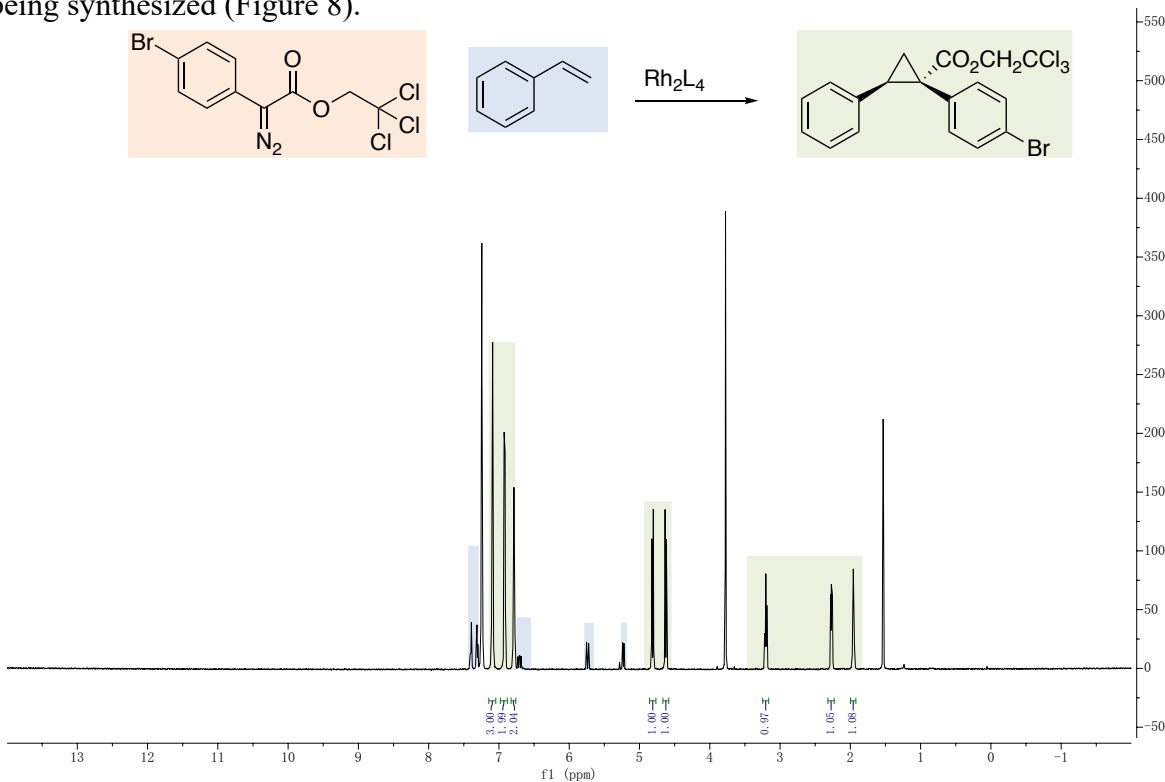


Figure 8: Analysis of Crude NMR

The diazo concentration was normalized and graphed against time on Microsoft Excel ® to show the relative rates of diazo decomposition (Figure 9).

Diazo Decomposition with Time

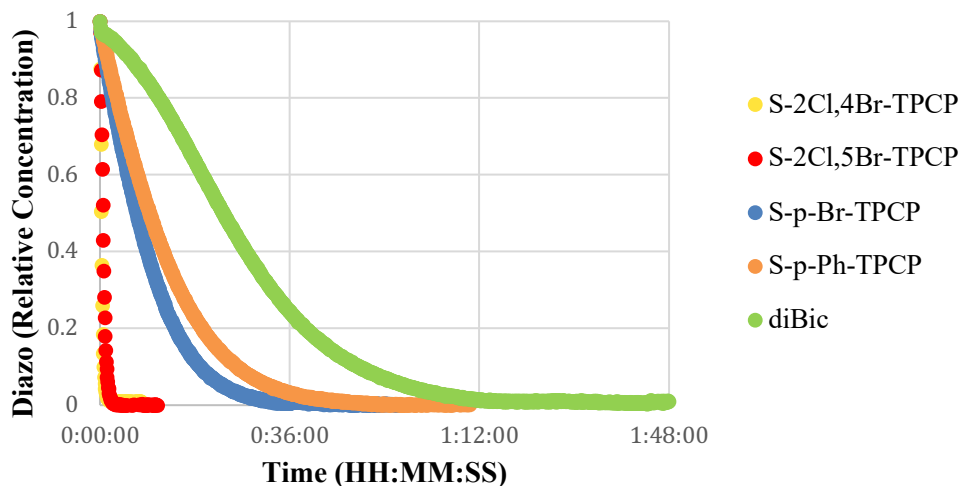


Figure 9: Relative Rates of Diazo Decomposition with Time

With the bulkier ligands, in the case of the $\text{Rh}_2(3,5\text{-di}(p\text{-tBuPh})\text{-TPCP})_4$, shown above as diBic, the rate of diazo decomposition slows down compared to the other catalysts with less bulky ligands. The percent yields and enantioselectivities of the experiments are tabulated below (Table 1).

Table 1: Enantioselectivities of Cyclopropane Products from Relative Rate Study

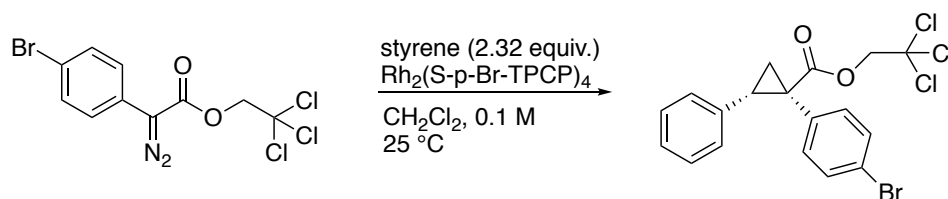
| Catalyst | Yield (%) | Enantioselectivity (% ee) |
|--------------------------------|-----------|---------------------------|
| (<i>S</i>)-(2-Cl, 4-Br)-TPCP | 83 | -29 |
| (<i>S</i>)-(2-Cl, 5-Br)-TPCP | 90 | -67 |
| (<i>S</i>)-p-Br-TPCP | 91 | 84 |
| (<i>S</i>)-p-Ph-TPCP | 89 | 80 |
| 3,5-di(<i>p</i> -tBuPh)-TPCP | 88 | -6 |

Not only did the $\text{Rh}_2(\text{diBic})_4$ catalyst experiment have the slowest rate of diazo decomposition, it also had a low % ee. Another trend in the reactivities and enantioselectivities which can be

concluded from the results shown in Figure 8 and Table 1, apart from $\text{Rh}_2(\text{diBic})_4$, is the faster the catalyst, the lower the enantioselectivity.

2.1.2) Catalyst Concentration Dependence and Catalyst Order

After understanding the relative reactivities and the performance of several triarylcyclopropane carboxylate catalysts, all further kinetic studies were completed with the catalyst that gave the highest enantioselectivity, the $\text{Rh}_2(\text{p-Br-TPCP})_4$ catalyst. To understand the effect of catalyst concentration on the reaction rate, the cyclopropanation reaction was completed with varying catalyst concentrations, from 0.005 mol% to 0.02 mol% (Figure 10).



Catalyst Concentration Dependence

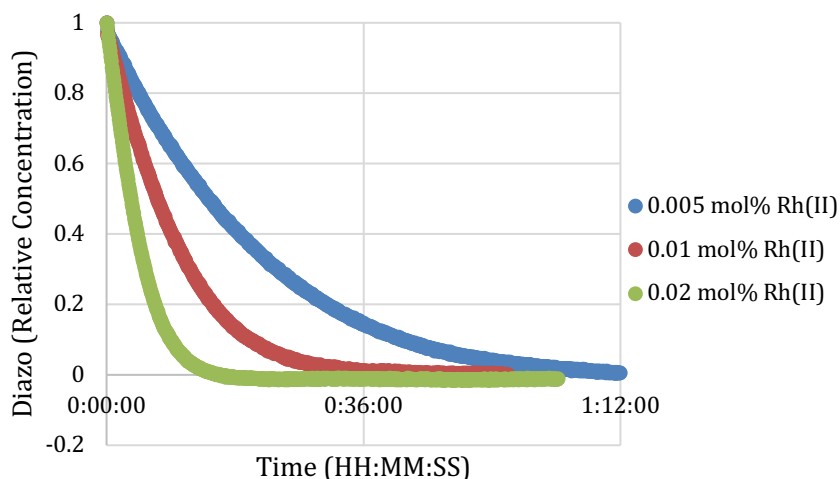


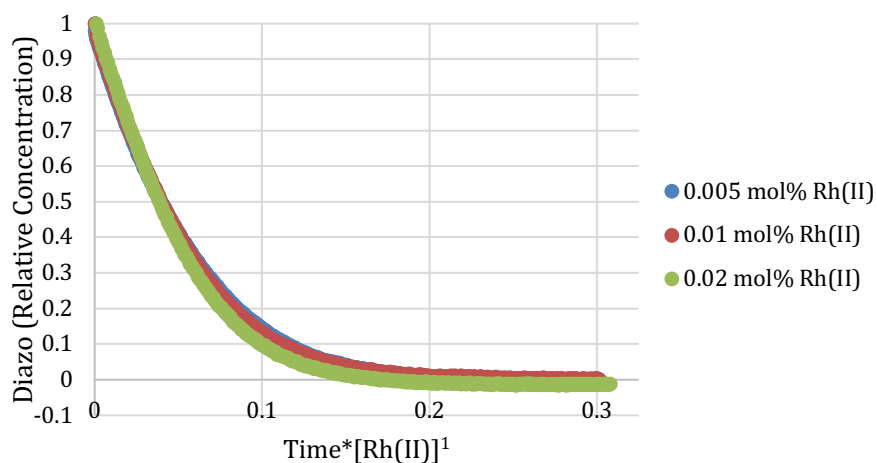
Figure 10: Catalyst Concentration Dependence Study

As predicted, the higher the concentration of catalyst, the faster the reaction rate; however, with the lower loading, not only is the rate of diazo decomposition slower, but the enantioselectivity also drops a significant amount, while the enantioselectivity is maintained with the higher concentration of catalyst (Table 2).

Table 2: Yields and Enantioselectivities for Catalyst Concentration Dependence Study

| Catalyst Loading | Yield (%) | Enantioselectivity (% ee) |
|------------------|-----------|---------------------------|
| 0.005 mol% | 85 | 60 |
| 0.01 mol% | 91 | 84 |
| 0.02 mol% | 86 | 85 |

Using the data from the catalyst concentration dependence study, the catalyst order was determined by Burés' method¹⁴. The diazo concentration data was plotted against a normalized time scale, $t[\text{cat}]_{\text{T}}^n$, where t is time, $[\text{cat}]_{\text{T}}$ is the total concentration of catalyst in the system, and n is the reaction order of catalyst. When the order of catalyst, n , was set to 1, a good overlap of all three curves can be seen (Figure 11).

Burés' Method for Determining Catalyst Order**Figure 11: Burés' Method for Determining Catalyst Order**

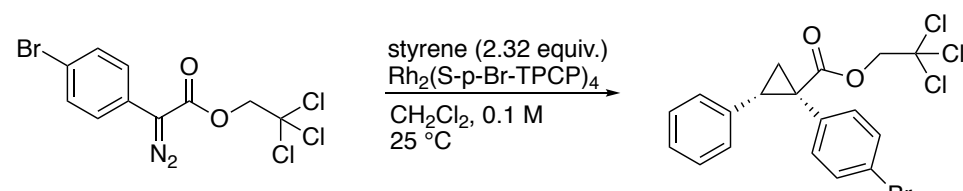
This overlap suggests the dirhodium-catalyzed cyclopropanation reaction is first order in catalyst.

2.2) Molecular Sieves as Drying Agent

The cyclopropanation reaction is very sensitive to air, with a possibility of O-H insertion as a side reaction, and under low loading, the catalyst is more susceptible to being poisoned by impurities; therefore, all reactions were completed under an atmosphere of argon, with the

reaction flask dried in the oven and cooled under vacuum before use. However, in the initial studies, the performances of the catalysts under the conditions in Figure 8 were variable between runs of the same experiment, especially when the slower, bulkier catalysts were used. A second-year graduate student in the group, Bo Wei, found that adding 4 Å molecular sieves as a drying agent helped overcome the inconsistency of data between runs with the same catalysts, as well as avoid a drop in enantioselectivity even at a catalyst loading of 0.0025 mol%; therefore, 4 Å molecular sieves were added to all subsequent experiments (Table 3).

Table 3: Enantioselectivities for Experiments with and Without Molecular Sieves



| Catalyst Loading | Without 4 Å MS | With 4 Å MS |
|------------------|----------------|-------------|
| 0.02 mol% | 85 | 94 |
| 0.01 mol% | 84 | 90 |
| 0.005 mol% | 60 | 92 |
| 0.0025 mol% | --- | 92 |

2.2.1) Relative Reactivities

The relative reactivities of the various catalysts from Figure 8 were tested again, with an additional catalyst added, the $\text{Rh}_2(2\text{-Cl-TPCP})_4$ catalyst, also known as the 2-Cl-TPCP, and the same trend in reactivities can be seen from Figure 9 where no molecular sieves were added (Figure 12).

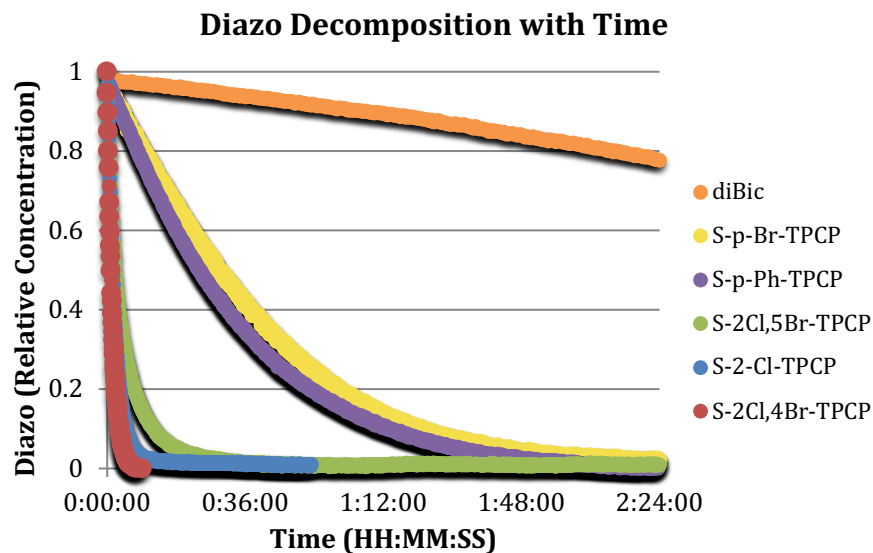


Figure 12: Relative Rates of Diazo Decomposition with Time, Molecular Sieves Added

Not only were the same relative reactivities observed, the enantioselectivity of the p-Br-TPCP catalyst also remained the highest among the six catalysts tested; therefore, it was used as the standard catalyst in further kinetics studies (Table 4).

Table 4: Enantioselectivities of Cyclopropane Products, with Molecular Sieves

$\xrightarrow[\text{MS } 4\text{\AA}]{\text{styrene (2.32 equiv.)}} \text{Rh}_2\text{L}_4 \text{ (0.0025 mol\%)}$
 $\text{CH}_2\text{Cl}_2, 0.1 \text{ M}$
 $25\text{ }^\circ\text{C}$

| Catalyst | Yield (%) | Enantioselectivity (% ee) |
|--------------------------------|-----------|---------------------------|
| 3,5-di(p-tBuPh)-TPCP | 90 | -21 |
| (<i>S</i>)-p-Br-TPCP | 92 | 92 |
| (<i>S</i>)-p-Ph-TPCP | 94 | -87 |
| (<i>S</i>)-(2-Cl, 5-Br)-TPCP | 84 | -38 |
| (<i>S</i>)-2-Cl-TPCP | 94 | 44 |
| (<i>S</i>)-(2-Cl, 4-Br)-TPCP | 81 | -37 |

2.2.2) Same Excess Experiment

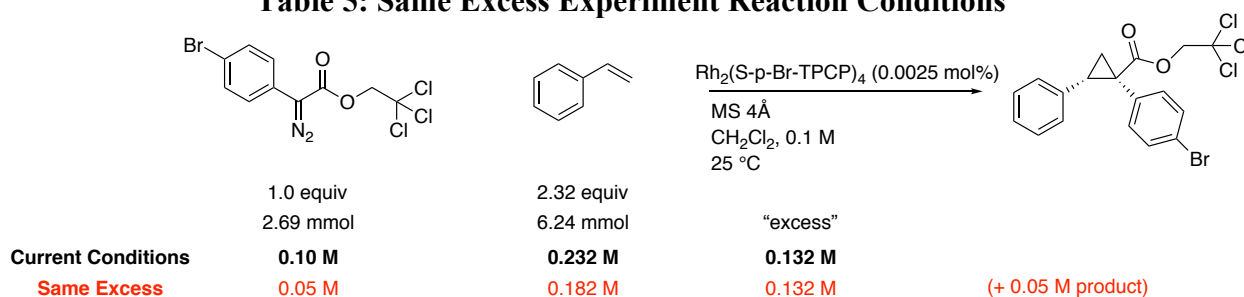
Once the standard conditions were set (catalyst loading, solvent and concentration, additives, and temperature), the second step of the RPKA, the “same excess” experiment, was

completed to probe the robustness of the rhodium (II) catalyst. In the same excess experiments, the reaction conditions at different time points are mimicked at the beginning of the reaction. The “excess” is the difference in concentration between the two substrates used, the diazo compound and styrene (Equation 2).

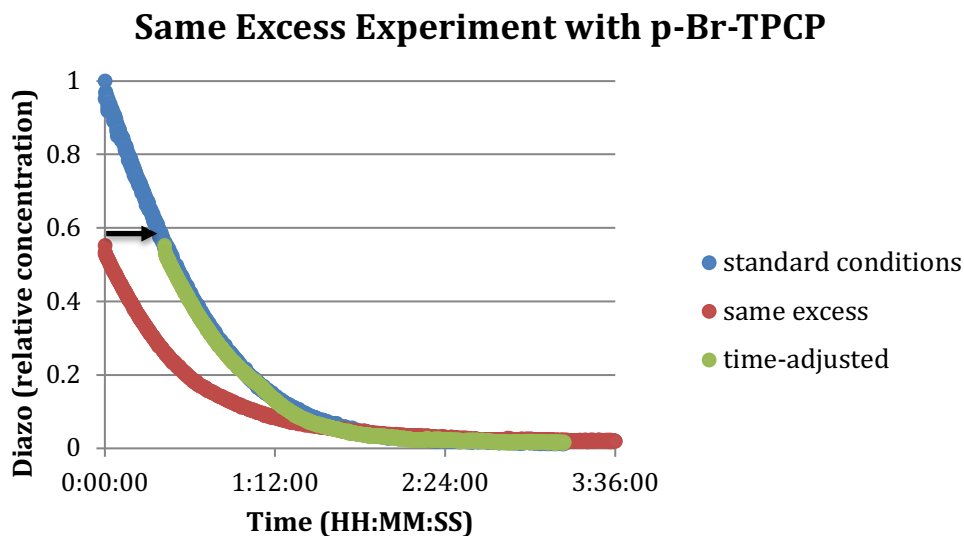
$$[xs] = [\text{styrene}] - [\text{diazo}] \quad (2)$$

In the same excess experiment, the [xs] should be the same as the amount in the standard conditions. If the catalyst is robust, there should be a good overlay of the same excess curve on top of the curve from the standard conditions. In this experiment, the reaction conditions at 50% conversion of the original reaction were mimicked (Table 5).

Table 5: Same Excess Experiment Reaction Conditions



At 50% conversion of the “Current Conditions,” half of the diazo had been converted into the cyclopropane product; therefore, in the “same excess experiment,” 0.05 molar of the cyclopropane product was added to the reaction system before adding catalyst. Based on this, the diazo decomposition was followed and graphed below, along with the curve from the standard conditions (Figure 13).



When the “same excess” curve is time-adjusted to start at the position of the standard conditions’ 50% conversion, a good overlap can be seen. The enantioselectivity is maintained even when mimicking the conditions at 50% conversion (Table 6).

Table 6: Yields and Enantioselectivities of Same Excess Experiment

| Condition | Yield (%) | Enantioselectivity (% ee) |
|-------------|-----------|---------------------------|
| Standard | 92 | 92 |
| Same Excess | 89 | 93 |

From the results seen in the “same excess” experiment, it can be concluded that the p-Br-TPCP catalyst is robust, where it completes the reaction without decomposing, and there is no inhibition of the catalyst by the product.

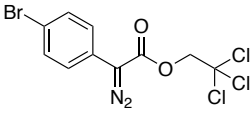
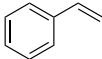
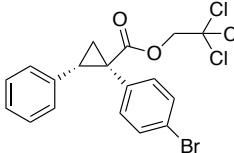
2.2.3) Different Excess Experiment

After determining that the catalyst is robust, the next step of the RPKA is to understand the concentration dependence of the other reactants in the system, which can lead to determining the reactant order, positive or negative. To achieve this, different excess experiments were completed. While the [xs] for the same excess experiment is equal to that of the [xs] in the

standard conditions, the different excess changes the concentration of one of the reagents, while keeping the other reagent's concentration the same as in the standard conditions, to create a different amount of [xs] in the experiment.

The first different excess experiment completed was with styrene, where the concentration of styrene was changed to create different amounts of excess (Table 7).

Table 7: Different Excess Reaction Conditions

| | | | | |
|---------------------------|---|---|--|---|
| |  |  | $\xrightarrow[\text{MS 4\AA}]{\text{Rh}_2(\text{p-Br-TPCP})_4 \text{ (0.0025 mol\%)}}$ CH ₂ Cl ₂ , 0.1 M 25 °C |  |
| | 1.0 equiv 2.69 mmol | 2.32 equiv 6.24 mmol | | |
| Current Conditions | 0.10 M | 0.232 M | "excess" | 0.132 M |
| Different Excess 1 | 0.10 M | 0.150 M | | 0.05 M |
| Different Excess 2 | 0.10 M | 0.175 M | | 0.075 M |

In the two "different excess" experiments, 0.150 and 0.175 molar of styrene were used, respectively, as opposed to the 0.232 molar in the standard conditions, while keeping the concentration of the diazo at 0.1 molar. The curves of the three experiments were graphed (Figure 14).

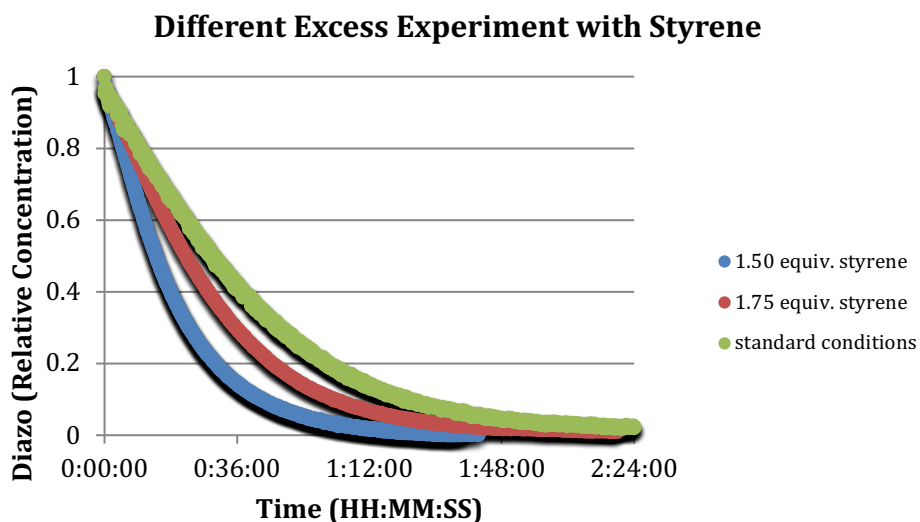


Figure 14: Different Excess Experiment with Styrene

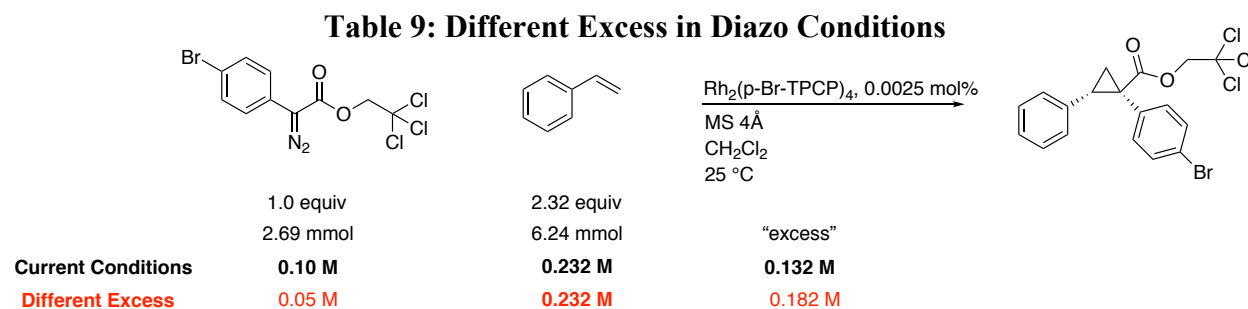
It was found that the lower the concentration of styrene, the faster the reaction rate; from this observation, it can be concluded qualitatively that the reaction is negative order with respect to styrene. However, the enantioselectivity drops with the decrease in styrene (Table 8).

Table 8: Yields and Enantioselectivities of Different Excess Experiments

| [Styrene] (M) | Yield (%) | Enantioselectivity (% ee) |
|---------------|-----------|---------------------------|
| 0.150 | 87 | 70 |
| 0.175 | 82 | 88 |
| 0.232 | 92 | 92 |

It was concluded that although the reaction rate slows down, giving a lower turnover number, the greater concentration of styrene gives a higher enantioselectivity because the styrene coordinates to the catalyst, stabilizing it.

A different excess experiment was completed with diazo, where the concentration of diazo was varied (Table 9).



To graph the data on, the concentration of diazo was converted into the concentration of styrene, where the "excess" amount in Table 9 was added to the values of the normalized IR response of the diazo decomposition (Figure 15).

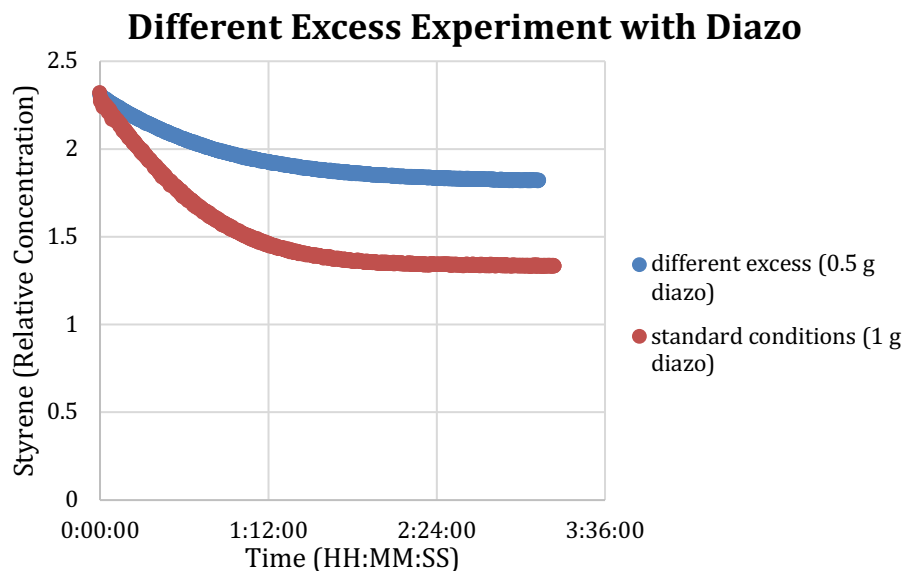


Figure 15: Different Excess Experiment- Styrene Decomposition with Time

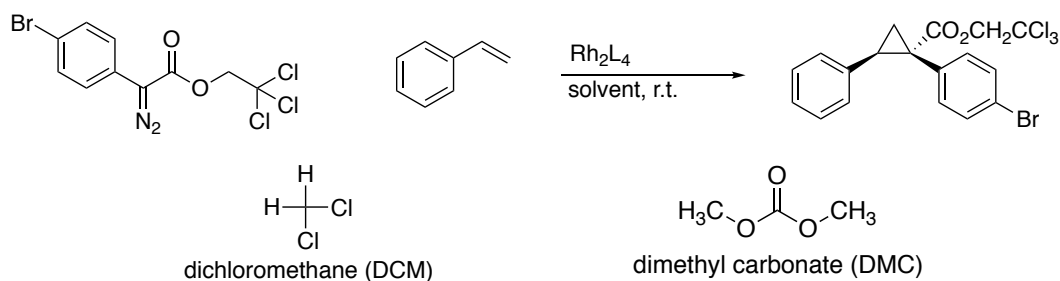
The rate of styrene consumption with the standard conditions is faster than the rate of styrene consumption with 0.05 molar diazo; this result qualitatively shows that the reaction has a positive order with respect to diazo. The yields and enantioselectivities for the different excess experiments are shown below (Table 10).

Table 10: Yields and Enantioselectivities for “Different Excess” Experiment in Diazo

| [Diazo] (M) | Yield (%) | Enantioselectivity (% ee) |
|-------------|-----------|---------------------------|
| 0.05 | 93 | 93 |
| 0.10 | 93 | 90 |

2.3) A Greener, Safer Solvent

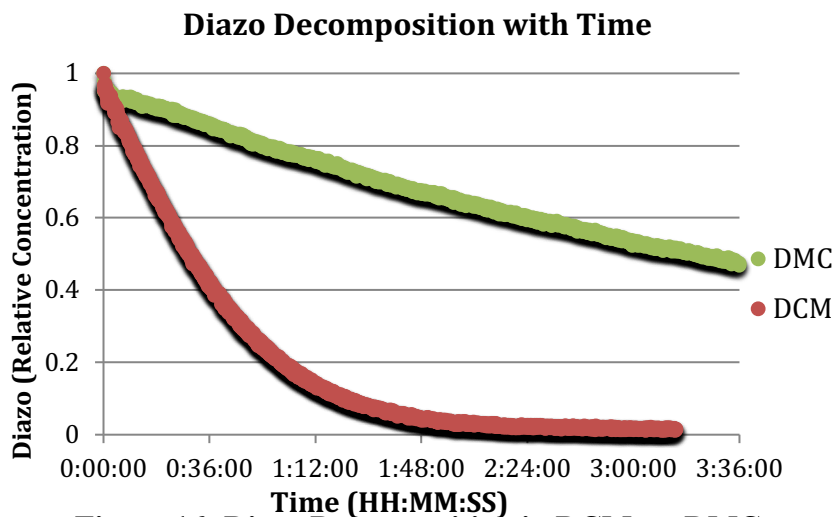
The standard conditions thus far use dichloromethane (DCM) as a solvent. Not only is DCM harmful to humans due to its high volatility, it is also very hard to dispose of because of its hazardous nature. Due to this factor, a summer rotation student, Jack Sharland, who is now a first-year student in the group, conducted studies of this cyclopropanation reaction with a less harmful, green solvent, dimethyl carbonate¹⁵ (DMC), where he screened many of the dirhodium catalysts available in the group, including some from this study (Table 11).

Table 11: Yields and Enantioselectivities in Dichloromethane vs. Dimethyl Carbonate

| Catalyst | % ee in DCM | % ee in DMC |
|---|-------------|-------------|
| $\text{Rh}_2(\text{S-DOSP})_4$ | -73 | -65 |
| $\text{Rh}_2(\text{R-PTAD})_4$ | 62% | 31 to 47% |
| $\text{Rh}_2(\text{S-TCPTAD})_4$ | -72% | -69 to -71% |
| $\text{Rh}_2(\text{S-2-Cl-TPCP})_4$ | 52% | 62% |
| $\text{Rh}_2(\text{S-2-Cl, 5-Br-TPCP})_4$ | 74% | 77% |
| $\text{Rh}_2(\text{S-p-Br-TPCP})_4$ | 91% | 95% |
| $\text{Rh}_2(\text{S-p-Ph-TPCP})_4$ | -94% | -97% |
| $\text{Rh}_2[(1R,2R)\text{-2-TMS-p-Br-DPCP}]_4$ | 86% | 97% |
| $\text{Rh}_2(\text{R-TPPTTL})_4$ | 90% | 95% |

Although some of the enantioselectivities decreased, the $\text{Rh}_2(\text{S-BTPCP})_4$ catalyst, and some of the other catalysts screened in previous experiments in this study, had improved enantioselectivities when DMC was used as the solvent. Therefore, the effect of solvent on this cyclopropanation system was further studied, along with an attempt to achieve a higher turnover number than what has been achieved thus far.

An experiment comparing DCM and DMC as a solvent was completed at a catalyst loading of 0.0025 mol% (Figure 16).



Although the rate of diazo decomposition in DMC was significantly slower than the rate in DCM, where the reaction was complete within four hours, the enantioselectivity of the product from the cyclopropanation in DMC was higher than that in DCM (Table 12).

Table 12: Yields and Enantioselectivities of Cyclopropane Product, DCM vs. DMC

| Solvent | Yield (%) | Enantioselectivity (% ee) |
|---------|-----------|---------------------------|
| DMC | --- | 97 |
| DCM | 92 | 92 |

Because the enantioselectivity increased, and the boiling point of DMC is higher (90 °C) than that of DCM (39.6 °C), it was decided that DMC would be used in further studies, especially with the higher turnover number attempts due to the possibility of increasing the temperature at lower catalyst loadings.

2.3.1) Varying Temperature

In Figure 16, the cyclopropanation reaction did not reach complete conversion in 36 hours, so the reaction was stopped. However, due to the higher enantioselectivity and the higher boiling point of DMC versus DCM, the reaction scheme below was tested again in DMC at varying temperatures to try and achieve complete conversion (Figure 17).

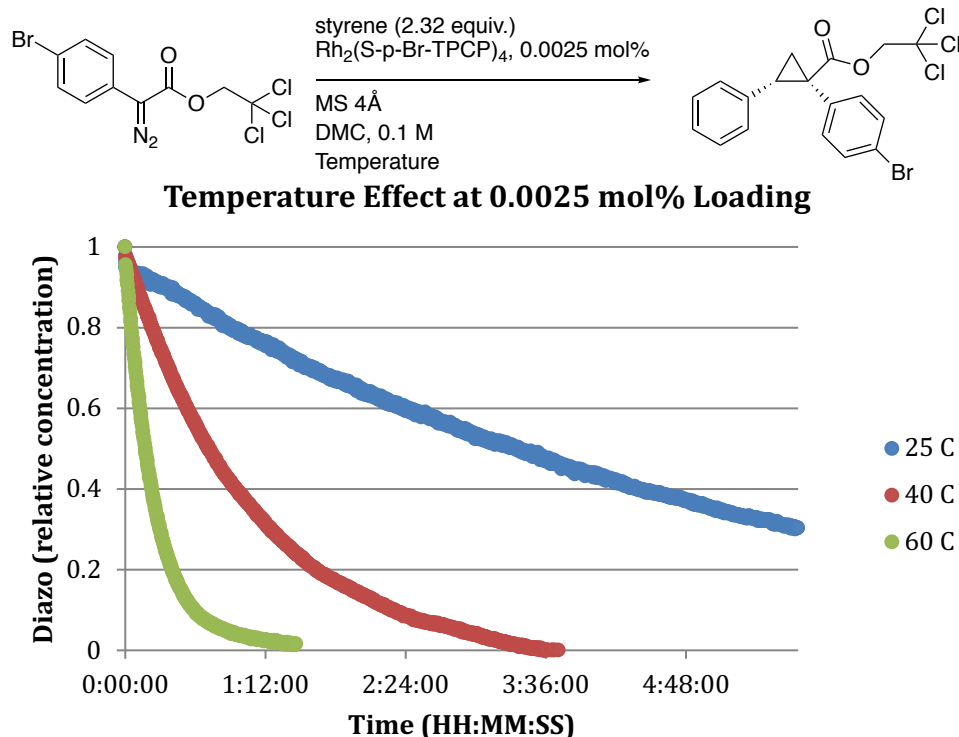


Figure 17: Temperature Effect at 0.0025 mol% Loading with DMC

As expected, the higher the temperature, the faster the reaction rate, and the cyclopropanation reaction was able to finish within four hours at 40 °C, and two hours at 60 °C. Although the enantioselectivity drops slightly with higher temperature, the enantioselectivities maintain a value around 95% (Table 13).

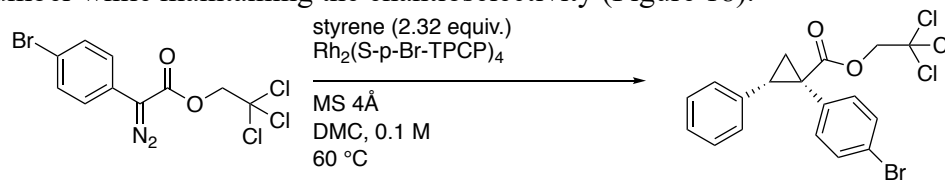
Table 13: Yields and Enantioselectivities of Temperature Effect Experiments

| Temperature (°C) | Yield (%) | Enantioselectivity (% ee) |
|------------------|-----------|---------------------------|
| 25 | --- | 97 |
| 40 | 72 | 96 |
| 60 | 88 | 95 |

2.3.2) Changing Catalyst Loading at 60 °C

Since the diazo decomposition graph reaches approximately zero within two hours at 60 °C, while maintaining a high level of enantioselectivity, further experiments were ran at 60 °C,

but this time, the catalyst loading was lowered with each experiment to try to achieve a higher turnover number while maintaining the enantioselectivity (Figure 18).



Changing Catalyst Loading at 60 °C

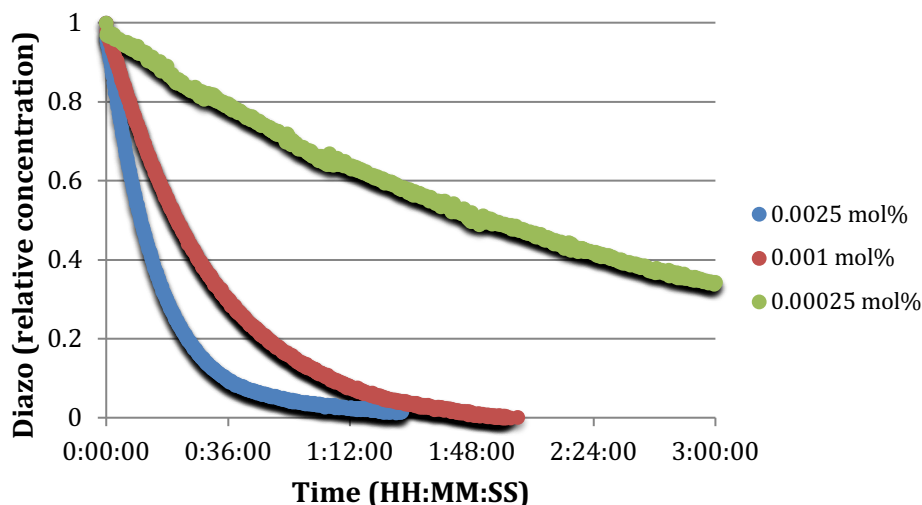


Figure 18: Changing Catalyst Loading at 60 °C

When the catalyst loading was decreased, the rate of the reaction slowed down significantly, especially at 0.00025 mol%; although not shown in Figure 18, the reaction with 0.00025 mol% catalyst does reach completion after 20 hours, however. The enantioselectivity is maintained at 95% ee even at a catalyst loading of 0.001 mol%, but drops down to 90% ee when 0.00025 mol% catalyst is used (Table 14).

Table 14: Yields and Enantioselectivities for Catalyst Loading Experiments

| Catalyst Loading | Yield (%) | Enantioselectivity (% ee) |
|------------------|-----------|---------------------------|
| 0.0025 mol% | 88 | 95 |
| 0.001 mol% | 89 | 95 |
| 0.00025 mol% | 90 | 90 |

2.3.3) One-Million Turnover Numbers

Although the enantioselectivity drops to 90% ee with 0.00025 mol% catalyst loading, the reaction still finishes within a reasonable time frame (under 24 hours); therefore, further experiments were ran at lower loadings and higher temperatures to try to achieve one million turnover numbers, a catalyst loading of 0.0001 mol% (Figure 19).

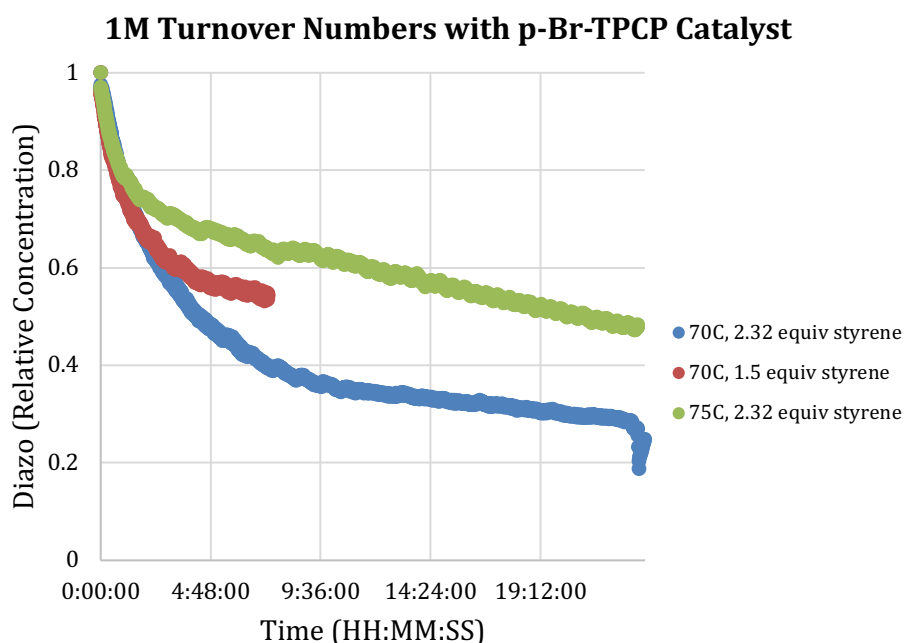
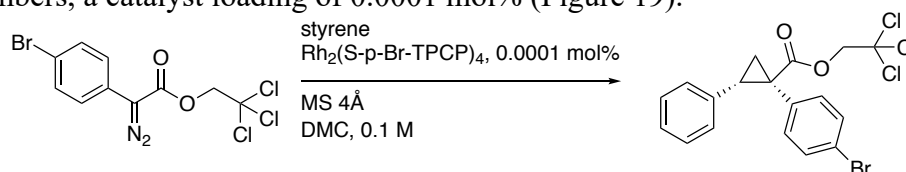


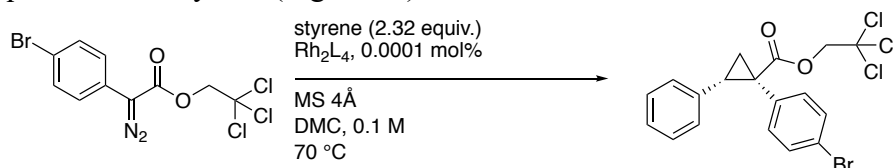
Figure 19: One-million Turnover Numbers with p-Br-TPCP Catalyst

The temperature or concentration of styrene used were varied, in some cases both were varied, to try to achieve complete conversion of the diazo into the cyclopropane product. However, none of the experiments were able to go to completion. The enantioselectivities were taken of the cyclopropane products that were formed from two of the experiments, but a significant drop in % ee from the higher catalyst loadings was observed (Table 15).

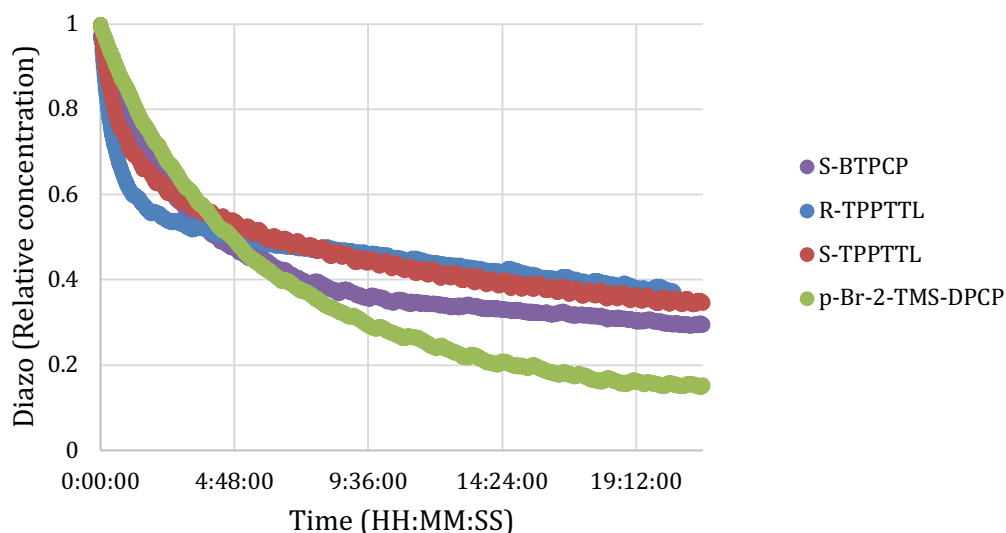
Table 15: Enantioselectivities of Cyclopropane Products

| Temperature (°C) | [Styrene] (M) | Enantioselectivity (% ee) |
|------------------|---------------|---------------------------|
| 70 | 0.150 | 79 |
| 70 | 0.232 | 79 |

Other catalysts available in the group, including two phthalamido ligand catalysts, were tested to see if one-million turnover numbers were possible under the following conditions: 70C, DMC, 2.32 equivalents of styrene (Figure 20).



1M Turnover Numbers with Different Catalyst

**Figure 20: One-million Turnover Numbers with Different Catalysts**

None of the catalysts tested were able to reach complete conversion of diazo, although a catalyst developed by a graduate student in the group, Benjamin Wertz, did come close, and had the highest level of enantioselectivity observed (Table 16).

Table 16: Enantioselectivities of Cyclopropane Products with Other Catalysts

| Catalyst | Enantioselectivity (% ee) |
|---|---------------------------|
| <i>S</i> -p-Br-TPCP | 79 |
| <i>R</i> -TPPTTL | -27 |
| <i>S</i> -TPPTTL | 58 |
| (<i>1S,2S</i>)- <i>p</i> -Br-2-TMS-DPCP | 87 |

2.3.4) Same Excess Experiment

Once the optimized conditions (temperature and catalyst loading) were identified for DMC as the solvent, the same excess experiments were completed again with DMC as the solvent to double-check the robustness of the catalyst (Figure 21).

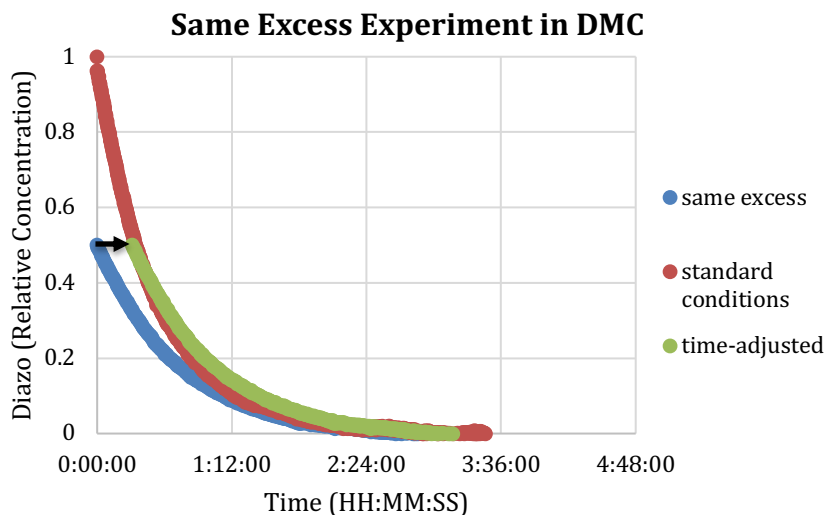
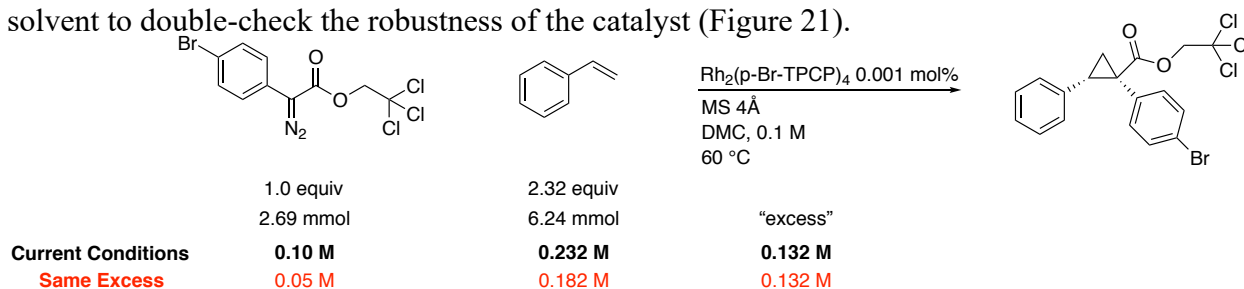


Figure 21: Same Excess Experiment with DMC as Solvent

As with DCM, there is a good overlap of the two curves when the same excess curve is time-adjusted to where the standard conditions curve is at 50% conversion, confirming the robustness of the catalyst even in DMC. Not only does the curve overlap well, the enantioselectivity is also

kept above 90% ee, showing that the p-Br-TPCP catalyst is robust even with DMC as the solvent (Table 17).

Table 17: Yields and Enantioselectivities for Same Excess Experiment in DMC

| Condition | Yield (%) | Enantioselectivity (% ee) |
|-------------|-----------|---------------------------|
| Standard | 89 | 95 |
| Same Excess | 92 | 92 |

2.3.5) Different Excess Experiments

Once the robustness of the catalyst in DMC was confirmed, the different excess experiments were completed.

The concentration of the styrene was set at 0.150 and 0.464 molar in the two experiments (Figure 22).

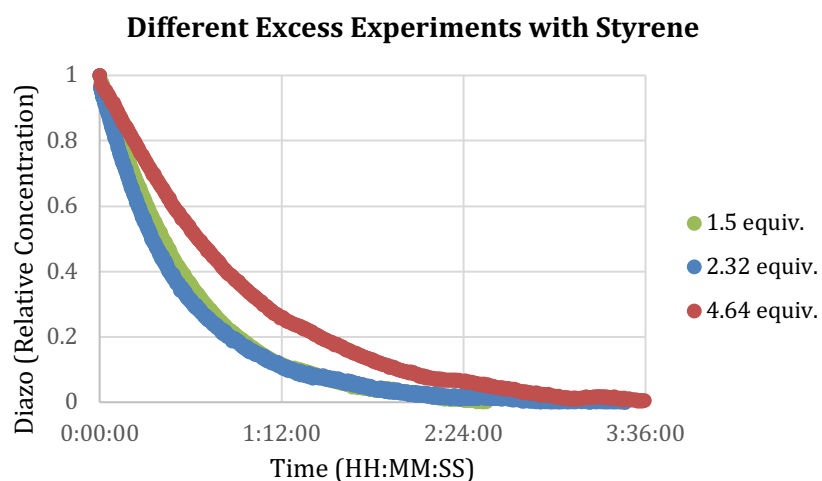
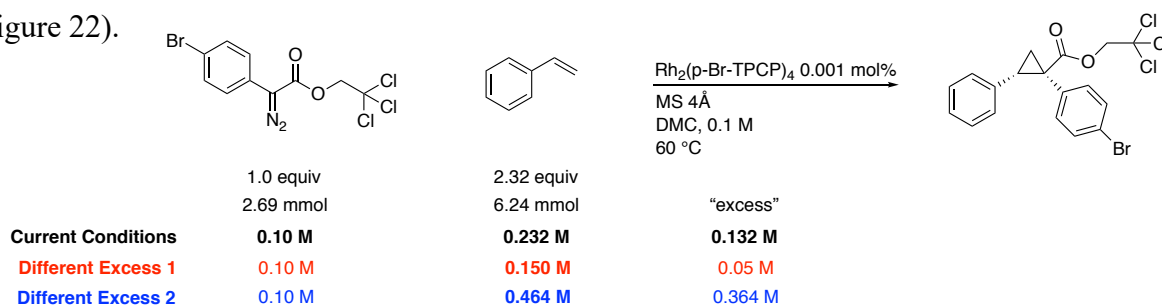


Figure 22: Different Excess Experiment with Styrene

The diazo decomposition curve of the different excess experiment with 1.5 equivalents of styrene overlaps well with the curve of the standard conditions (2.32 equivalents), but the

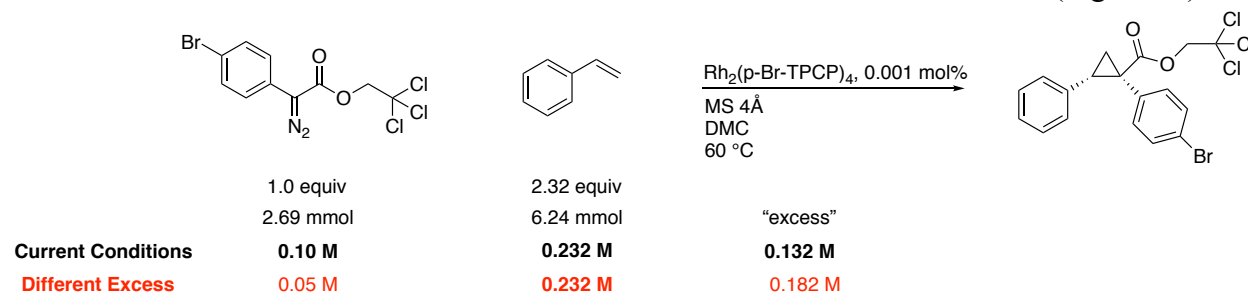
enantioselectivities of the two non-standard conditions are lower than that of the standard conditions (Table 18).

Table 18: Yields and Enantioselectivities of Different Excess Experiments with Styrene

| [Styrene] (M) | Yield (%) | Enantioselectivity (% ee) |
|---------------|-----------|---------------------------|
| 0.150 | 88 | 92 |
| 0.232 | 89 | 95 |
| 0.464 | 90 | 90 |

Further analysis is currently being done to understand these results.

The different excess experiment with diazo was done in the same way as the one in DCM, where the concentration of diazo was varied from 0.1 molar to 0.05 molar (Figure 23).



Different Excess Experiment with Diazo

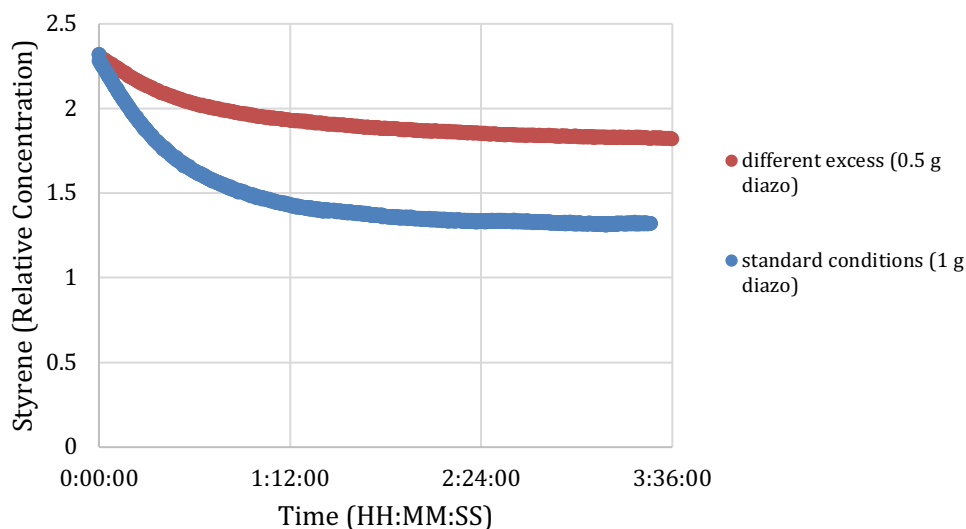


Figure 23: Different Excess Experiment with Diazo

Like with DCM as the solvent, the rate of diazo consumption is faster when there is more diazo in the system (standard conditions) compared to the experiment with 0.05 molar diazo.

Qualitatively, this confirms that the reaction is positive order with respect to the diazo. With less diazo, the enantioselectivity drops slightly, but still maintains a level above 90% ee (Table 19).

Table 19: Yields and Enantioselectivities for Different Excess with Diazo

| [Diazo] (M) | Yield (%) | Enantioselectivity (% ee) |
|-------------|-----------|---------------------------|
| 0.05 | 89 | 92 |
| 0.10 | 89 | 95 |

2.4) Discussion

The different studies reported above studied the cyclopropanation reaction of trichloroethyl ester diazoacetates with styrene catalyzed by the rhodium (II) triarylcyclopropane carboxylate catalysts. The studies were done by in situ IR studies using ReactIR™, and the diazo decomposition curve (peak 2103 cm⁻¹) was monitored to produce these results.

The first set of studies, section 2.1, conducted preliminary kinetics studies on the catalysts to understand the general reactivities of the catalysts with different ligands, finding that the bulkier the ligands, such as Rh₂(diBic)₄, catalyzed the reaction more slowly. The relative reactivities study showed that although not the fastest, the p-Br-TPCP catalyst gave the highest level of enantioselectivity (84% ee). Using the Burés method, it was determined that the cyclopropanation reaction is first order in catalyst, found by the good overlap of the three curves obtained from experiments with different catalyst loadings.

The second set of studies, section 2.2, further optimized the reaction conditions, by adding molecular sieves to produce consistent results between experiments with the same catalysts and reaction conditions. Further studies beyond the relative reactivities, including the same excess and different excess experiments, were conducted. Through these two “excess”

studies with the p-Br-TPCP catalyst, it was found that the catalyst is robust and maintains structural integrity throughout the course of the reaction, and the reaction has a negative order in styrene and a positive order in the diazo compound.

Inspired by the solvent system studies conducted by a graduate student in the group, the third set of studies, section 2.3, looked to using dimethyl carbonate (DMC) as a greener alternative to dichloromethane (DCM). It was found that not only did the reactions in DMC give higher levels of enantioselectivities (97% in DMC versus 92% in DCM), it also opened up the possibility to conduct reactions in higher temperatures and lower loadings of catalyst due to the higher boiling point of DMC compared to that of DCM. The rhodium (II)-catalyzed cyclopropanation reaction was studied at various temperatures, from 25 °C to 60 °C, even to 75 °C when trying to achieve one-million turnover numbers (TON). At 60 °C, it was found that the level of enantioselectivity was maintained even at a catalyst loading of 0.001 mol% (95% ee), so the catalyst loading was lowered while maintaining the reaction temperature at 60 °C. Although it is currently not possible to achieve one-million TON while maintaining a high level of enantioselectivity under the various sets of conditions, even with different generation catalysts available in the group, the robustness of the p-Br-TPCP catalyst at low catalyst loading (>0.0001 mol%) was confirmed.

3) Conclusions

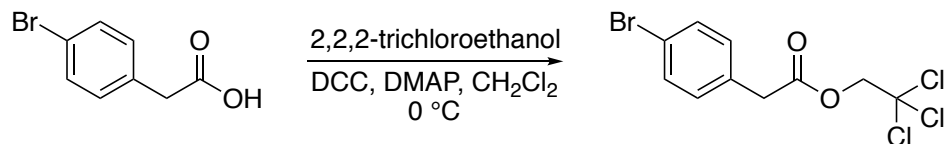
The rhodium (II)-catalyzed cyclopropanation reaction was optimized using *in situ* infrared spectroscopy studies to understand the effect of catalyst ligands on the performance of the catalyst. It was found that, of all the catalysts screened in this study, $\text{Rh}_2(\text{p-Br-TPCP})_4$ catalyst gave the highest enantioselectivity in both DCM and DMC, with and without molecular sieves (97% ee in DMC with molecular sieves). Further studies following the RPKA model found that the rhodium catalyst is robust, where the product does not inhibit catalytic activity, and the reaction is first order in catalyst, negative order in styrene, and positive order in diazo. Although one-million TON was not achieved in the scope of this study, low catalyst loading conditions in a green solvent, DMC, were found to be possible, leading to efficient and practical use of the rhodium (II) catalysts in cyclopropanation reactions. Application of high TON conditions to other different olefins and carbene precursors, as well as other reactions, such as tandem cyclopropanation/ Cope rearrangement and ylide-induced cascade reactions, will be explored in the future.

4) Experimental

4.1) General Remarks

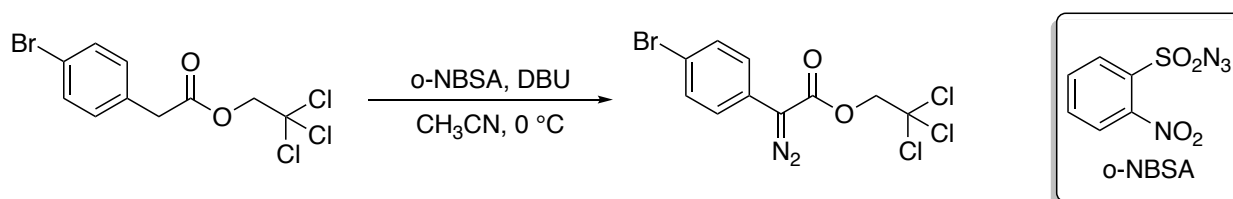
All experiments were carried out in oven-dried glassware under argon atmosphere. Flash column chromatography was performed on silica gel. All solvents were distilled using a short-path distillation system the day before or the same day when the reactions were completed. Molecular sieves (4Å) were activated under vacuum at 300 °C over 3 hours and stored in the oven. *In situ* IR experiments were carried out with the Mettler Toledo ReactIR™ 45m instrument. All chemicals were obtained commercially. Styrene was filtered through silica before each experiment. ¹H NMR spectra were obtained on a 400 and 600 MHz spectrometer in deuterated chloroform (CDCl₃), with residual chloroform taken as an internal standard (7.26 ppm for ¹H, and 77.23 ppm for ¹³C), and were reported in parts per million (ppm). The abbreviations for multiplicity are as follows: s= singlet, d= doublet, t= triplet, q= quartet, p= pentet, m= multiplet, dd= doublet of doublet, etc. Coupling constants (J values) are obtained from the spectra. TLC was done on aluminum-back silica gel plates with UV light to visualize.

4.2) General Procedure for Synthesis of Diazo Compounds



2,2,2-trichloroethyl 2-(4-bromophenyl)acetate: 4-bromophenylacetic acid (15 g, 1.0 equiv.), N,N-dimethyl 4-aminopyridine [DMAP] (0.85 g, 0.1 equiv.), and 2,2,2-trichloroethanol (8 mL, 1.2 equiv.) were dissolved in 150 mL CH₂Cl₂ and the solution cooled to 0 °C. A solution of N,N-dicyclohexylcarbodiimide [DCC] (15.9 g, 1.1 equiv.) in CH₂Cl₂ (75 mL) was added to the reaction mixture via an addition funnel over 5 minutes. The reaction mixture was allowed to stir

overnight at room temperature. The reaction mixture was filtered by vacuum filtration over a pad of celite and washed with Et₂O (100 mL). The filtrate was concentrated to give a yellow oil that solidified under high vacuum. The product was used without further purification to synthesize the diazo compound.



2,2,2-trichloroethyl 2-(4-bromophenyl)-2-diazoacetate: The ester from above (11 g, 1.0 equiv.) and *o*-NBSA (11 g, 1.5 equiv.) were dissolved in acetonitrile (318 mL), and the solution was cooled to 0 °C. DBU (9.5 mL, 2.0 equiv.) was added dropwise via a syringe. The reaction mixture was allowed to stir for 1 hour at 0 °C. The reaction mixture was then quenched with saturated aqueous NH₄Cl and extracted with Et₂O three times. The organic layer was washed with H₂O and brine, dried over MgSO₄, and filtered. The filtrate was filtered over a silica plug and eluted with 6% Et₂O in pentane. The solvent was removed in vacuo and further purified via column chromatography (Biotage). The orange fractions were collected and combined, and the solvent was removed in vacuo and put under high vacuum overnight to give the product as an orange crystalline solid. ¹H NMR (400 MHz; CDCl₃) δ 7.57-7.51 (m, 2H), 7.42-7.36 (m, 2H), 4.92 (s, 2H). The ¹H NMR data matched the literature data¹⁶.

4.3) General Procedure of ReactIR™ Set-up and Cyclopropanation Reactions

The ReactIR™ instrument was filled with liquid nitrogen and allowed to equilibrate while the reaction flask was being set-up. An oven-dried 100 mL 3-neck round-bottom flask with 4 Å

molecular sieves was fitted with a rubber septum (left neck, 14/20), ReactIR™ probe (center neck, 24/40 to 19/25 adapter, 19/25 neck), and argon inlet (right neck, 14/20) (Figure 24).



Figure 24: *In Situ* IR Apparatus Set-up

The flask was cooled to room temperature under vacuum, and then backfilled with argon. The flask was placed in a water or oil bath, with the temperature of the stir plate set to the desired temperature and stir rate on 700 rpm. Once the reaction flask was at the desired temperature, the background and water vapor spectrum were taken via the ReactIR™ instrument. The syringe and needle used for the solvent was primed with argon from the flask before adding solvent through the rubber septum. The data collection was started on the software, and the solvent was allowed to stir for 15 minutes. After a reference spectrum of the solvent was taken, styrene was added using a plastic syringe. The reaction mixture was allowed to stir while the diazo carbonyl compound was weighed out. A reference spectrum of styrene was taken after subtracting out the solvent spectrum, and then the diazo compound was added by removing and quickly replacing the rubber septum. A reference spectrum was taken of the diazo compound after subtracting out the reference spectrum of styrene, and the reaction mixture was allowed to stir for 15 minutes. 1 mL of the catalyst stock solution (created by measuring out the calculated amount of catalyst,

dissolved in 25 mL of solvent, then 1 mL of the 25 mL was taken out and diluted to 10 mL to create the catalyst stock solution) was added to the reaction mixture and allowed to stir until the complete consumption of the diazo compound, determined by the diazo stretching frequency (2103 cm^{-1}).

4.4) General Procedure for ReactIR™ Data Analysis

The completed diazo decomposition graph on the ReactIR™ software is shown below (Figure

25).

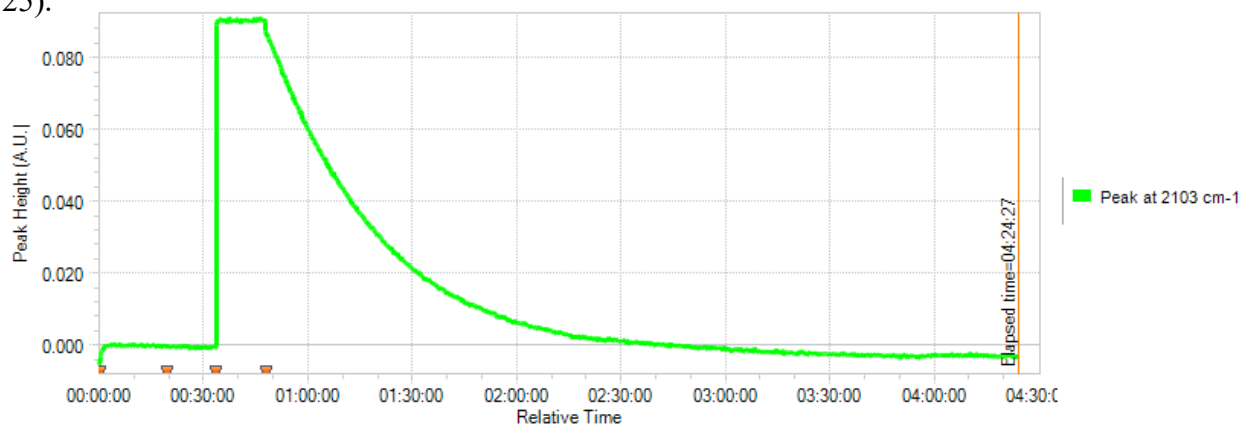
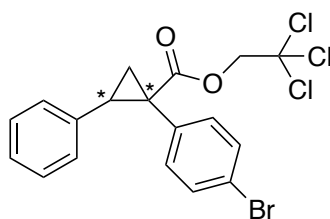


Figure 25: ReactIR™ Run on Software for A Complete Experiment

The data was extracted directly from the software as a text-file and copied into Microsoft Excel®. The point at which the curve rises sharply at a right angle, around the 30-minute mark, is where the diazo carbonyl compound was added to the reaction mixture. The catalyst solution was injected where the curve starts to decrease, around the 45-minute mark. The absorbance point and relative time at which the catalyst was added, all the way until the end of the data collection period, was set as the beginning of the diazo decomposition curve. The first time point in the diazo decomposition curve is set as “00:00:00” (HH:MM:SS) by subtracting the relative time at that point from itself, and all subsequent time points are set by subtracting the relative time of the beginning of the data set from the relative time extracted from Figure 24. To

normalize the absorbance, the absorbance of the first point in the data set is set as “1,” which is obtained from dividing the absorbance of the first point by itself, and all subsequent absorbances are divided by the absorbance of the first point. In doing so, it is possible to get the relative concentration of diazo and to monitor the time of the diazo decomposition.

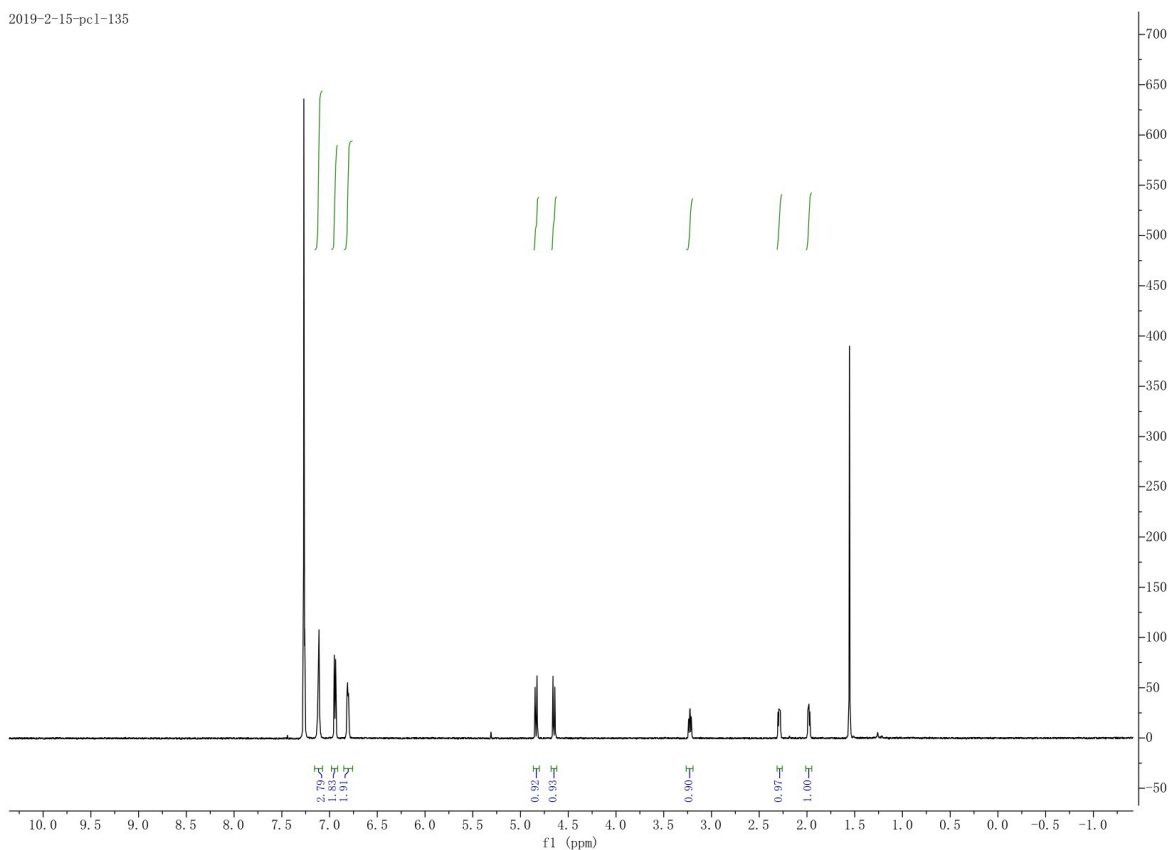
4.5) Analysis of Cyclopropane Products



2,2,2-trichloroethyl 1-(4-bromophenyl)-2-phenylcyclopropane-1-carboxylate:

$^1\text{H NMR}$ (600 MHz; CDCl_3) δ 7.27-7.24 (m, 2H), 7.13-7.08 (m, 3H), 6.95- 6.91 (m, 2H), 6.83-

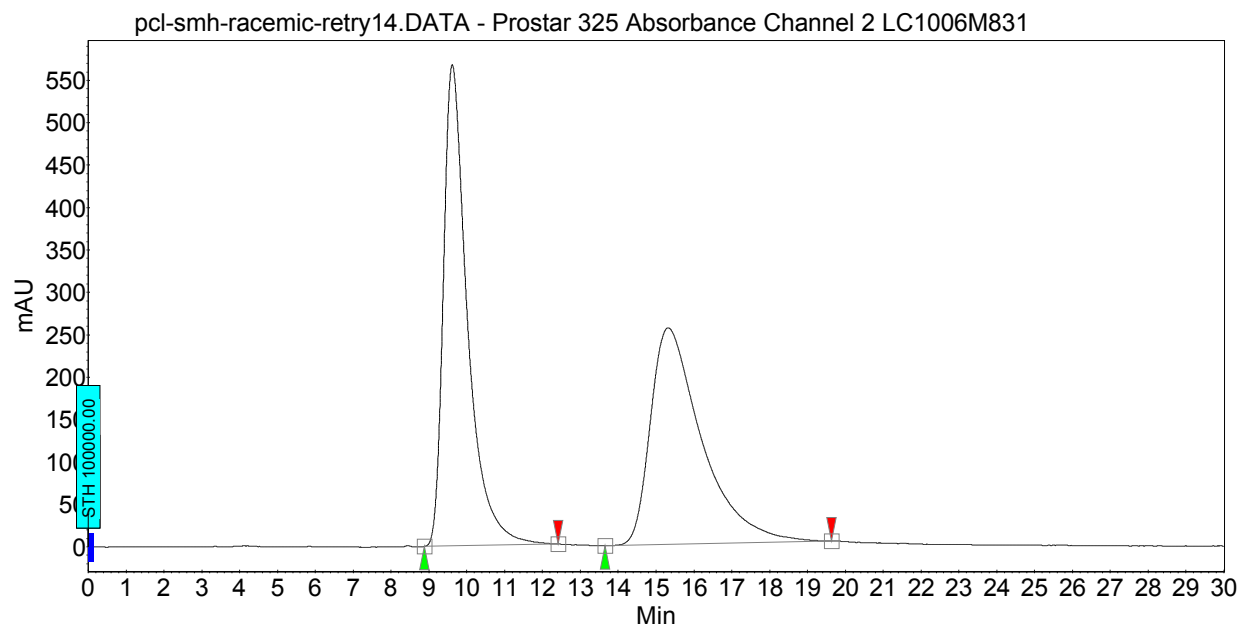
2019-2-15-pc1-135



4.6) HPLC Traces

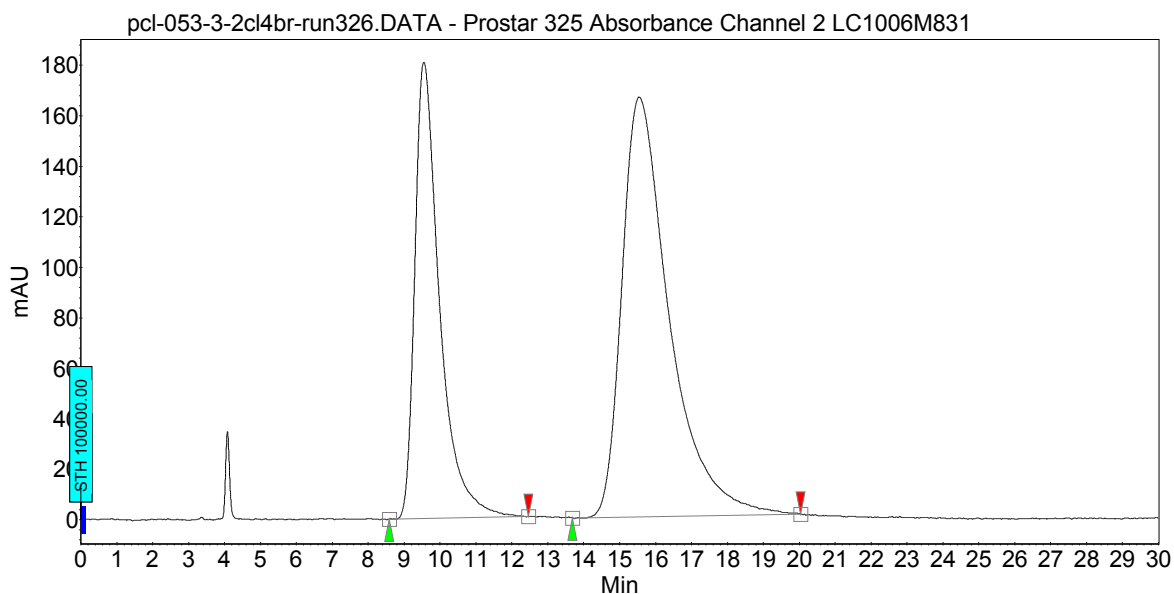
Data relevant to **Section 2.1**

Rh₂(OAc)₄ racemic



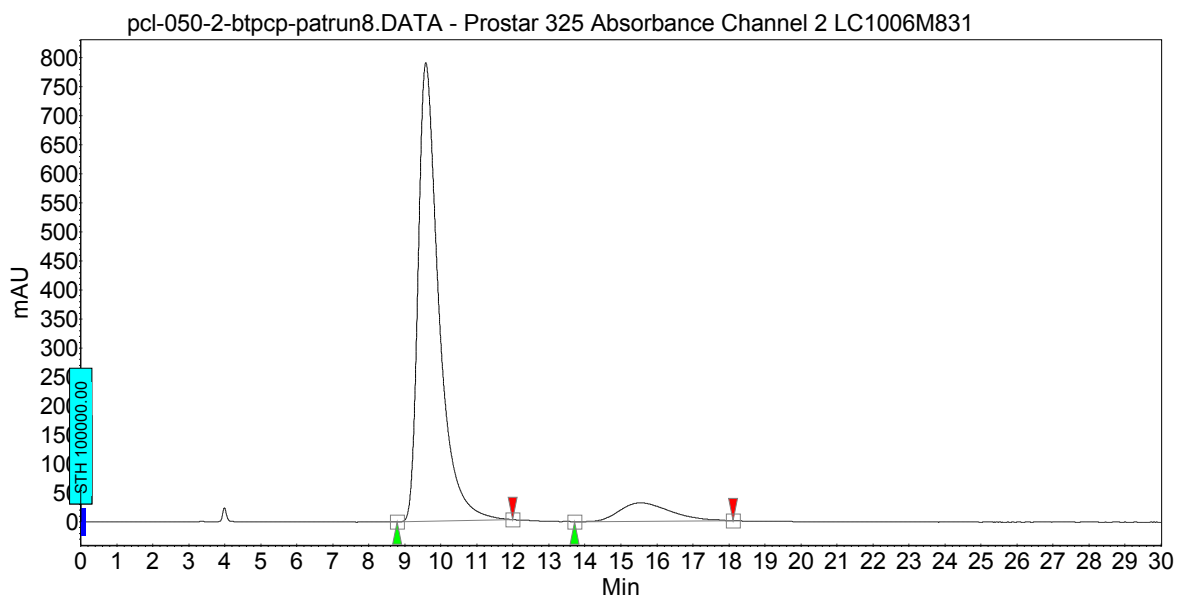
Peak results :

| Index | Name | Time [Min] | Quantity [% Area] | Height [mAU] | Area [mAU.Min] | Area % [%] |
|-------|---------|------------|-------------------|--------------|----------------|------------|
| 1 | UNKNOWN | 9.62 | 51.13 | 567.0 | 417.4 | 51.133 |
| 2 | UNKNOWN | 15.32 | 48.87 | 255.1 | 398.9 | 48.867 |
| Total | | | 100.00 | 822.1 | 816.3 | 100.000 |



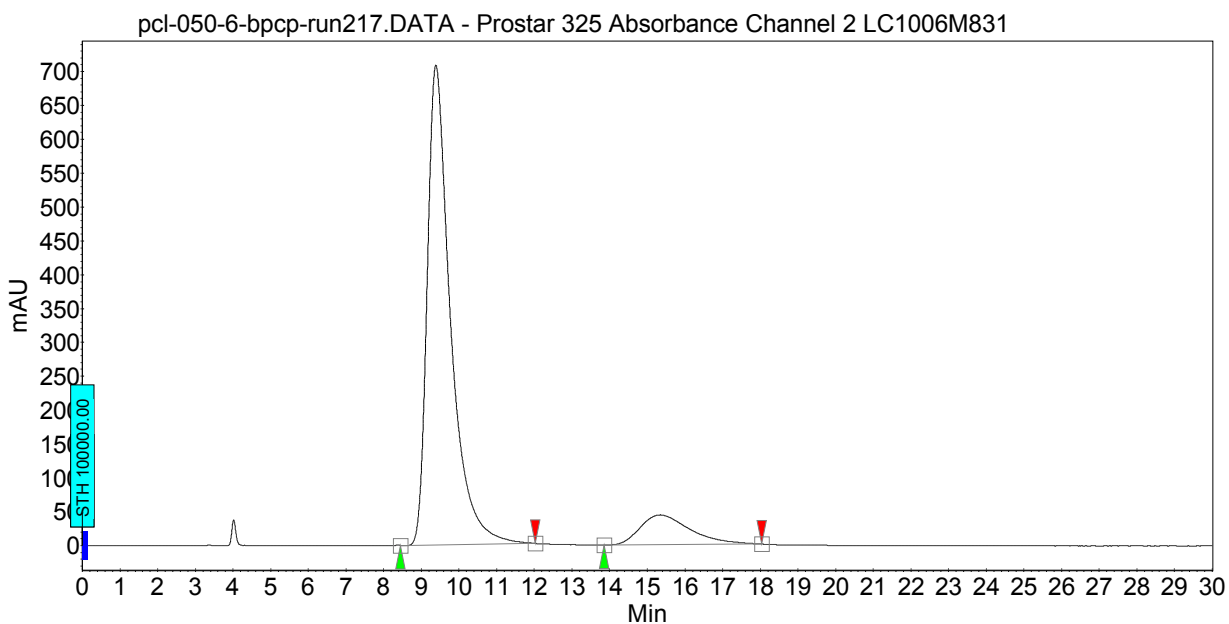
Peak results :

| Index | Name | Time [Min] | Quantity [% Area] | Height [mAU] | Area [mAU.Min] | Area % [%] |
|-------|---------|------------|-------------------|--------------|----------------|------------|
| 1 | UNKNOWN | 9.55 | 36.31 | 180.7 | 144.3 | 36.307 |
| 2 | UNKNOWN | 15.54 | 63.69 | 166.2 | 253.1 | 63.693 |
| Total | | | 100.00 | 346.9 | 397.4 | 100.000 |



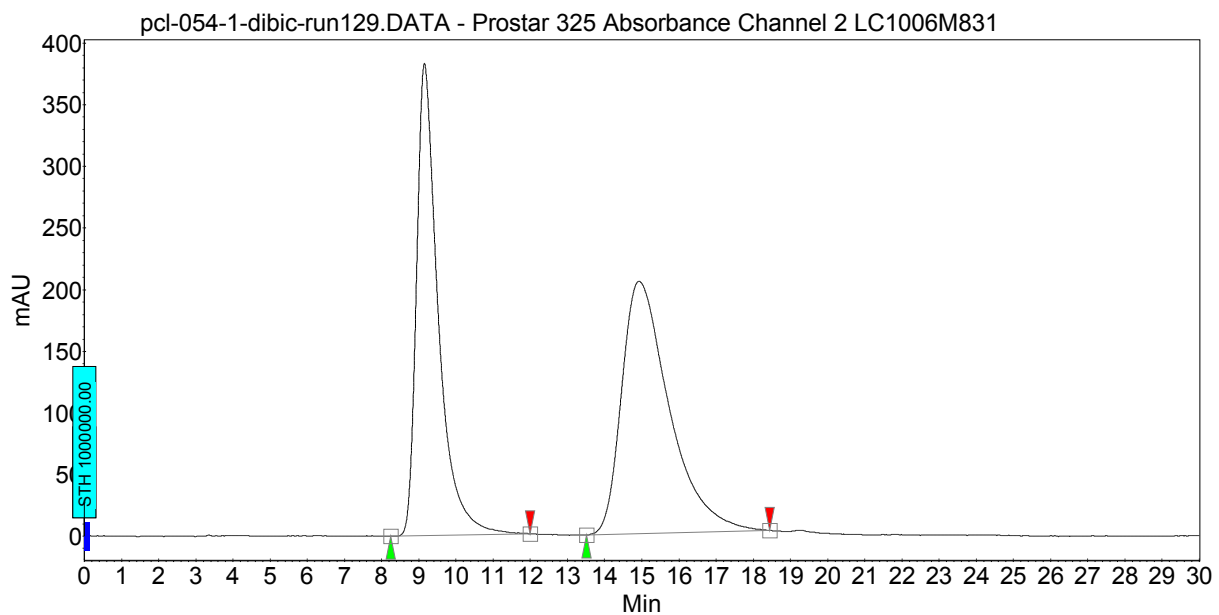
Peak results :

| Index | Name | Time [Min] | Quantity [% Area] | Height [mAU] | Area [mAU.Min] | Area % [%] |
|-------|---------|------------|-------------------|--------------|----------------|------------|
| 1 | UNKNOWN | 9.58 | 90.84 | 790.4 | 523.8 | 90.843 |
| 2 | UNKNOWN | 15.58 | 9.16 | 31.8 | 52.8 | 9.157 |
| Total | | | 100.00 | 822.2 | 576.6 | 100.000 |



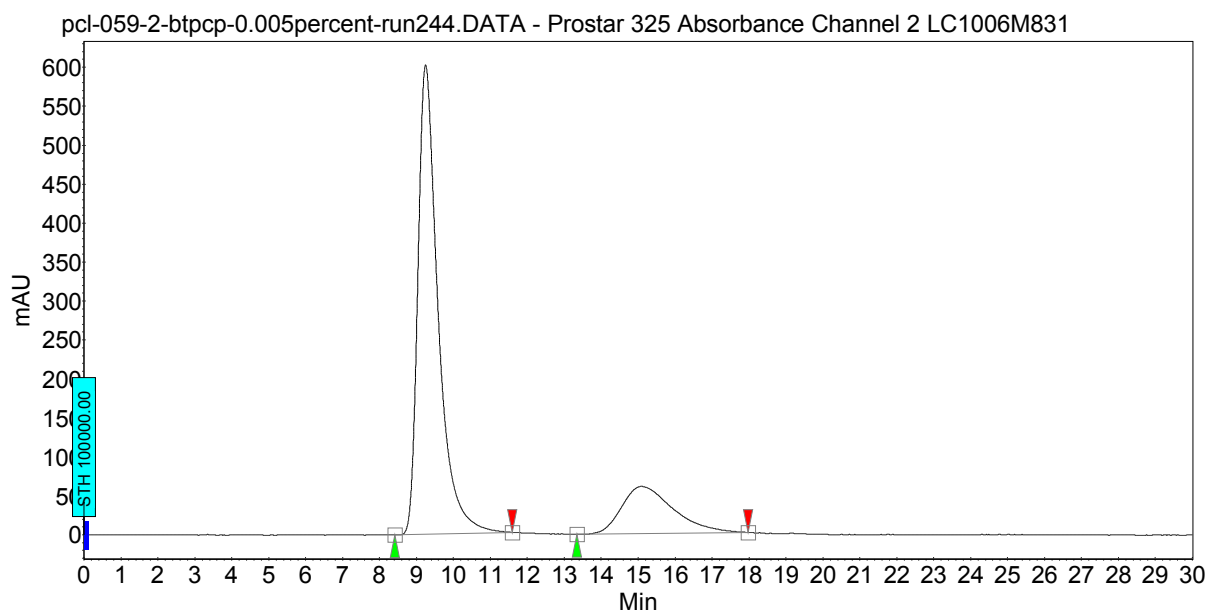
Peak results :

| Index | Name | Time [Min] | Quantity [% Area] | Height [mAU] | Area [mAU.Min] | Area % [%] |
|-------|---------|------------|-------------------|--------------|----------------|------------|
| 1 | UNKNOWN | 9.39 | 88.16 | 708.0 | 505.0 | 88.157 |
| 2 | UNKNOWN | 15.34 | 11.84 | 44.1 | 67.8 | 11.843 |
| Total | | | 100.00 | 752.1 | 572.8 | 100.000 |



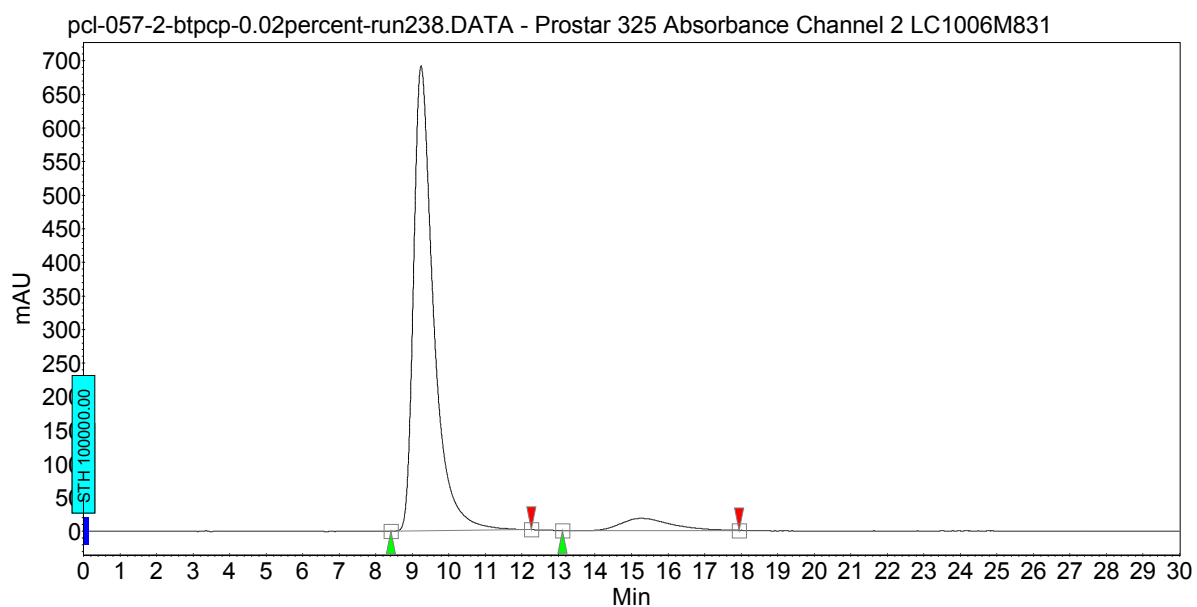
Peak results :

| Index | Name | Time [Min] | Quantity [% Area] | Height [mAU] | Area [mAU.Min] | Area % [%] |
|-------|---------|------------|-------------------|--------------|----------------|------------|
| 1 | UNKNOWN | 9.15 | 46.09 | 383.3 | 259.6 | 46.093 |
| 2 | UNKNOWN | 14.92 | 53.91 | 204.8 | 303.6 | 53.907 |
| Total | | | 100.00 | 588.1 | 563.3 | 100.000 |



Peak results :

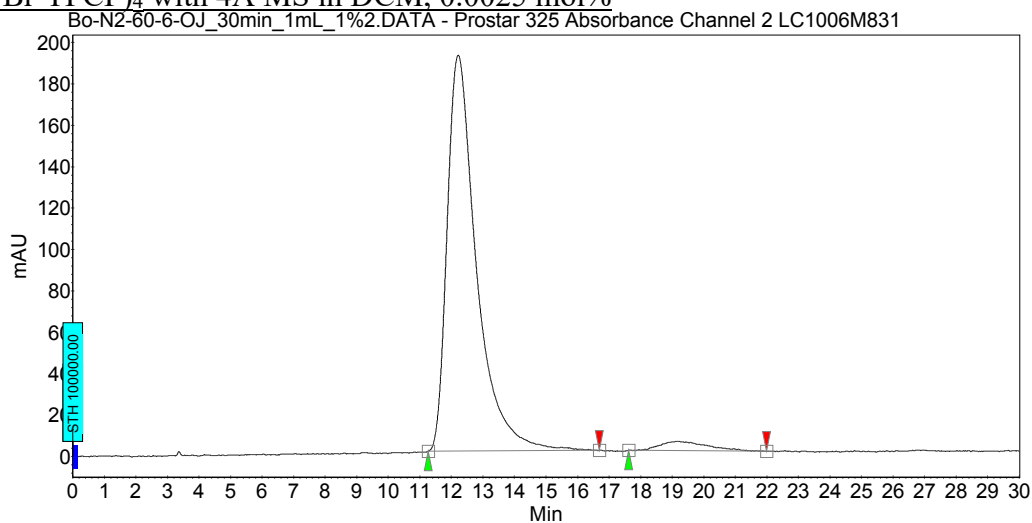
| Index | Name | Time [Min] | Quantity [% Area] | Height [mAU] | Area [mAU.Min] | Area % [%] |
|-------|---------|------------|-------------------|--------------|----------------|------------|
| 1 | UNKNOWN | 9.25 | 79.56 | 602.0 | 380.9 | 79.562 |
| 2 | UNKNOWN | 15.08 | 20.44 | 60.5 | 97.8 | 20.438 |
| Total | | | 100.00 | 662.5 | 478.7 | 100.000 |



Peak results :

| Index | Name | Time [Min] | Quantity [% Area] | Height [mAU] | Area [mAU.Min] | Area % [%] |
|-------|---------|------------|-------------------|--------------|----------------|------------|
| 1 | UNKNOWN | 9.24 | 93.83 | 691.6 | 436.4 | 93.831 |
| 2 | UNKNOWN | 15.26 | 6.17 | 18.1 | 28.7 | 6.169 |
| Total | | | 100.00 | 709.7 | 465.1 | 100.000 |

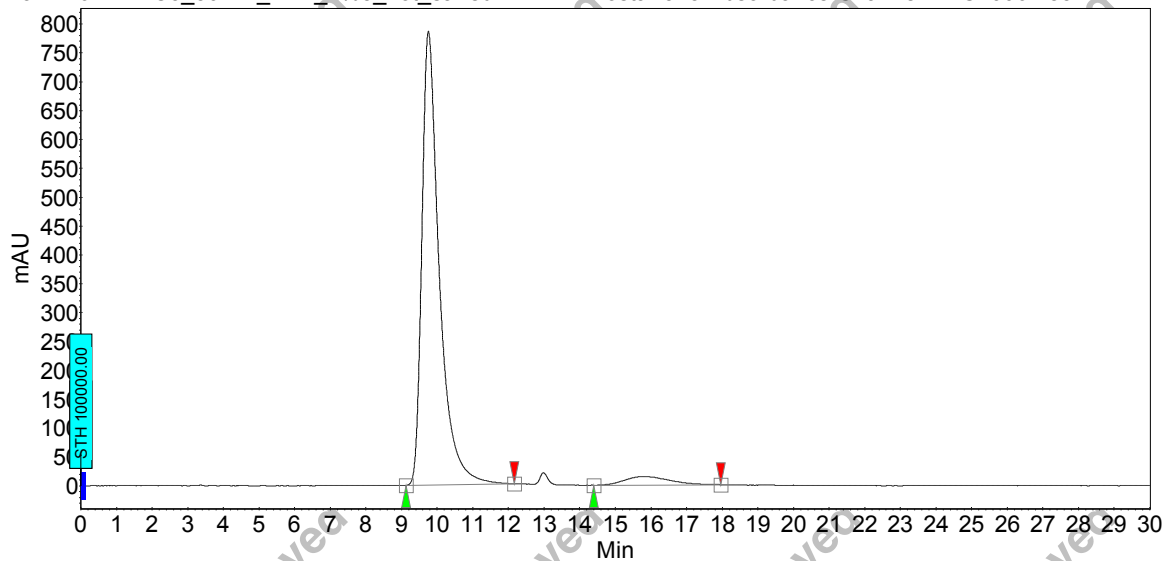
Data relevant to Section 2.2

Rh₂(S-p-Br-TPCP)₄ with 4Å MS in DCM, 0.0025 mol%**Peak results :**

| Index | Name | Time [Min] | Quantity [% Area] | Height [mAU] | Area [mAU.Min] | Area % [%] |
|-------|---------|------------|-------------------|--------------|----------------|------------|
| 1 | UNKNOWN | 12.22 | 96.31 | 191.2 | 206.0 | 96.311 |
| 2 | UNKNOWN | 19.13 | 3.69 | 4.5 | 7.9 | 3.689 |
| Total | | | 100.00 | 195.7 | 213.9 | 100.000 |

Same excess, DCM

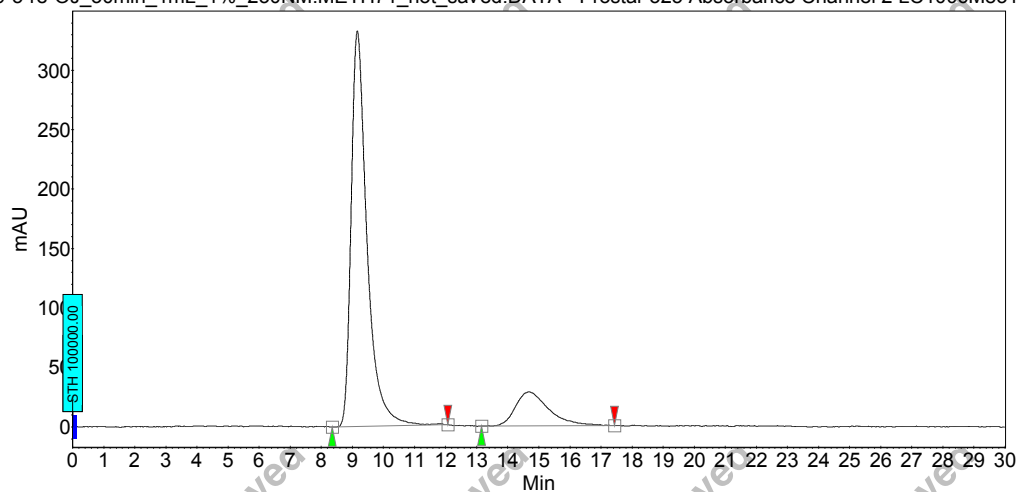
Bo-N2-61-4-2-OJ_30min_1mL_1%5_not_saved.DATA - Prostar 325 Absorbance Channel 2 LC1006M831

**Peak results :**

| Index | Name | Time [Min] | Quantity [% Area] | Height [mAU] | Area [mAU.Min] | Area % [%] |
|-------|---------|------------|-------------------|--------------|----------------|------------|
| 1 | UNKNOWN | 9.75 | 95.37 | 786.3 | 445.0 | 95.371 |
| 2 | UNKNOWN | 15.77 | 4.63 | 14.8 | 21.6 | 4.629 |
| Total | | | 100.00 | 801.1 | 466.6 | 100.000 |

Different excess in styrene, DCM: 1.5 equiv.

PCL-89-5-re-OJ_30min_1mL_1%_230NM.METH71_not_saved.DATA - Prostar 325 Absorbance Channel 2 LC1006M831

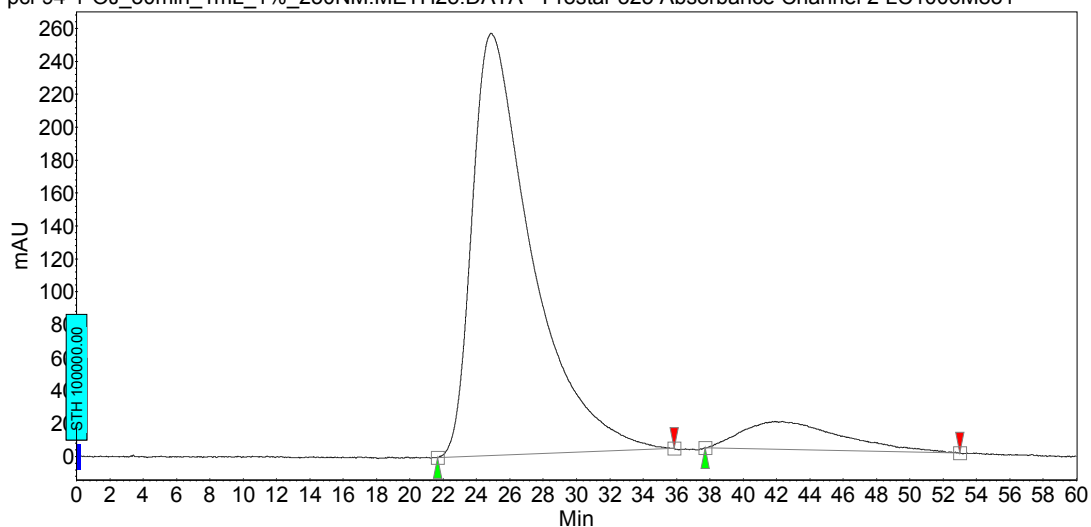


Peak results :

| Index | Name | Time [Min] | Quantity [% Area] | Height [mAU] | Area [mAU.Min] | Area % [%] |
|-------|---------|------------|-------------------|--------------|----------------|------------|
| 1 | UNKNOWN | 9.16 | 84.70 | 332.7 | 196.2 | 84.703 |
| 2 | UNKNOWN | 14.67 | 15.30 | 28.6 | 35.4 | 15.297 |
| Total | | | 100.00 | 361.3 | 231.7 | 100.000 |

Different excess in styrene, DCM: 1.75 equiv.

pcl-94-1-OJ_30min_1mL_1%_230NM.METH25.DATA - Prostar 325 Absorbance Channel 2 LC1006M831

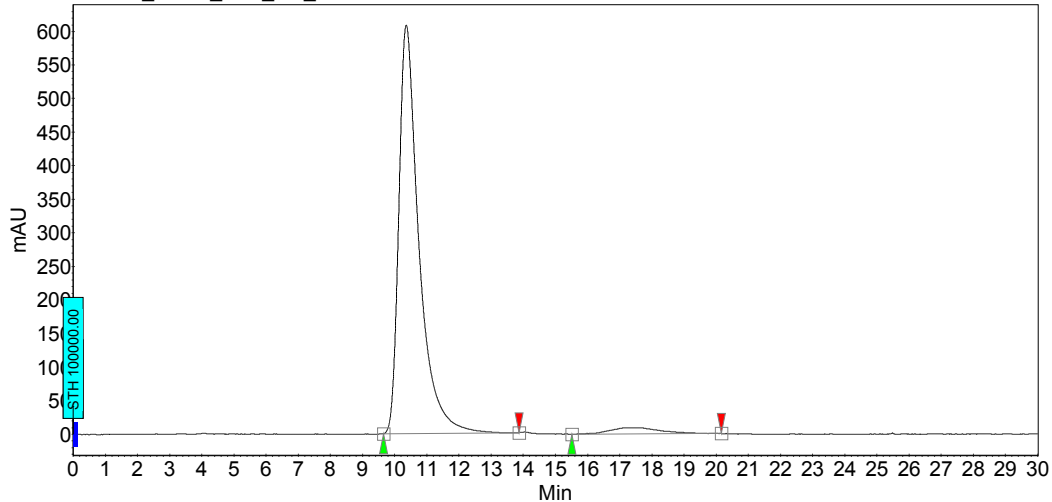


Peak results :

| Index | Name | Time [Min] | Quantity [% Area] | Height [mAU] | Area [mAU.Min] | Area % [%] |
|-------|---------|------------|-------------------|--------------|----------------|------------|
| 1 | UNKNOWN | 24.86 | 89.93 | 256.8 | 1062.6 | 89.931 |
| 2 | UNKNOWN | 42.36 | 10.07 | 17.0 | 119.0 | 10.069 |
| Total | | | 100.00 | 273.8 | 1181.6 | 100.000 |

Different excess in diazo, DCM: 0.5g diazo

Bo-N2-100-1-OJ_30min_1mL_1%_230NM.METH5.DATA - Prostar 325 Absorbance Channel 2 LC1006M831



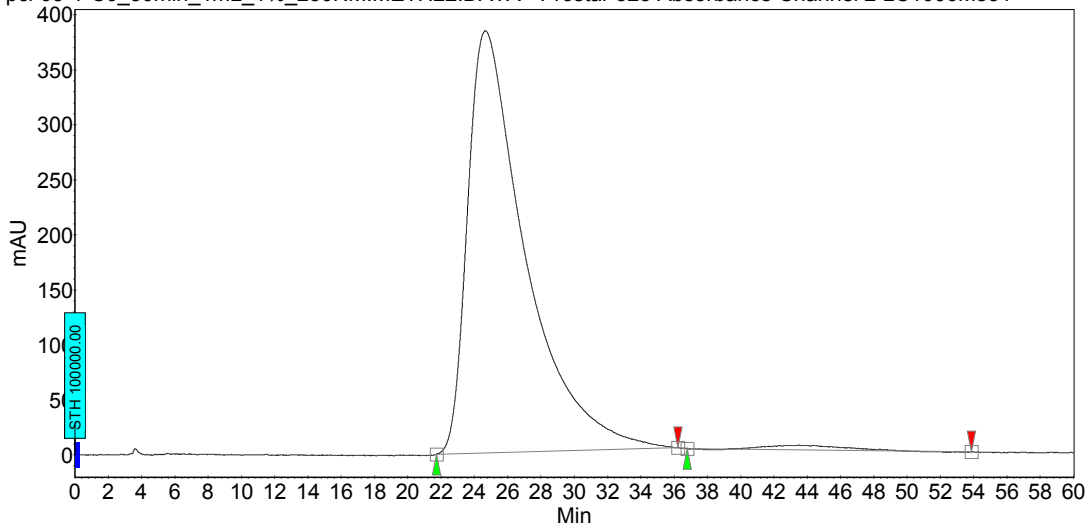
Peak results :

| Index | Name | Time [Min] | Quantity [% Area] | Height [mAU] | Area [mAU.Min] | Area % [%] |
|-------|---------|------------|-------------------|--------------|----------------|------------|
| 1 | UNKNOWN | 10.36 | 96.31 | 607.8 | 438.0 | 96.315 |
| 2 | UNKNOWN | 17.36 | 3.69 | 9.2 | 16.8 | 3.685 |
| Total | | | 100.00 | 617.0 | 454.8 | 100.000 |

Data relevant to Section 2.3

0.0025 mol% at 25 °C

pcl-93-1-OJ_30min_1mL_1%_230NM.METH22.DATA - Prostar 325 Absorbance Channel 2 LC1006M831

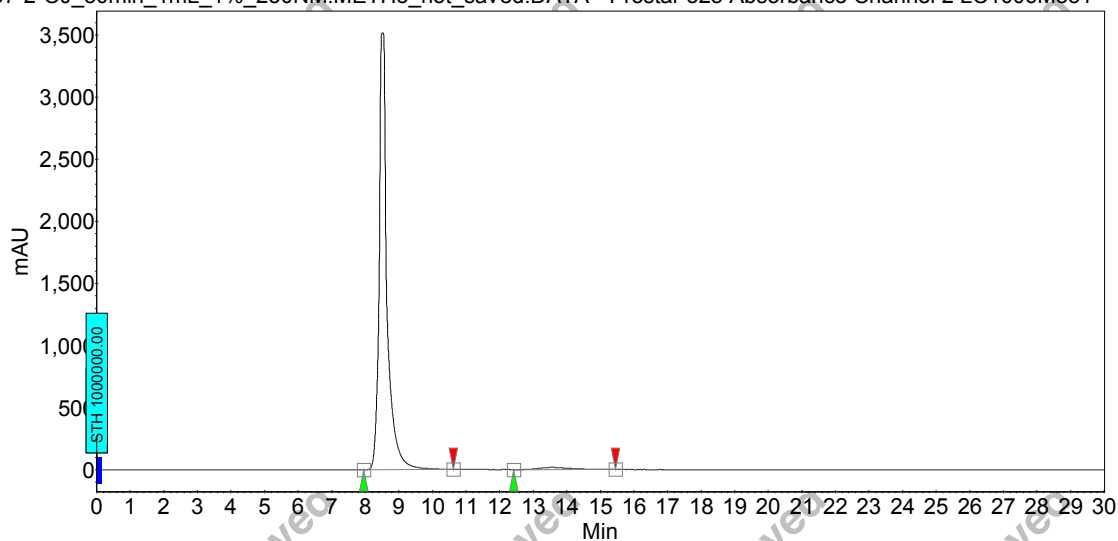


Peak results :

| Index | Name | Time [Min] | Quantity [% Area] | Height [mAU] | Area [mAU.Min] | Area % [%] |
|-------|---------|------------|-------------------|--------------|----------------|------------|
| 1 | UNKNOWN | 24.64 | 98.61 | 383.6 | 1541.0 | 98.613 |
| 2 | UNKNOWN | 43.54 | 1.39 | 4.3 | 21.7 | 1.387 |
| Total | | | 100.00 | 387.9 | 1562.7 | 100.000 |

0.0025 mol% at 40 °C

pcl-97-2-OJ_30min_1mL_1%_230NM.METH5_not_saved.DATA - Prostar 325 Absorbance Channel 2 LC1006M831

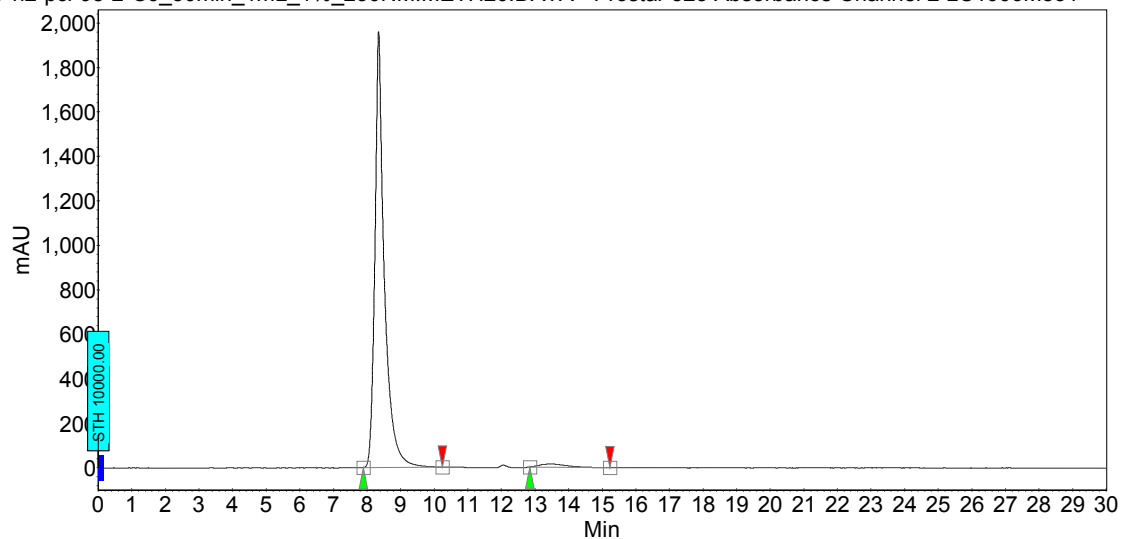


Peak results :

| Index | Name | Time [Min] | Quantity [% Area] | Height [mAU] | Area [mAU.Min] | Area % [%] |
|-------|---------|------------|-------------------|--------------|----------------|------------|
| 1 | UNKNOWN | 8.50 | 98.04 | 3513.7 | 970.8 | 98.040 |
| 2 | UNKNOWN | 13.54 | 1.96 | 17.5 | 19.4 | 1.960 |
| Total | | | 100.00 | 3531.2 | 990.2 | 100.000 |

0.0025 mol%, 60 °C

BO-n2-pcl-98-2-OJ_30min_1mL_1%_230NM.METH20.DATA - Prostar 325 Absorbance Channel 2 LC1006M831

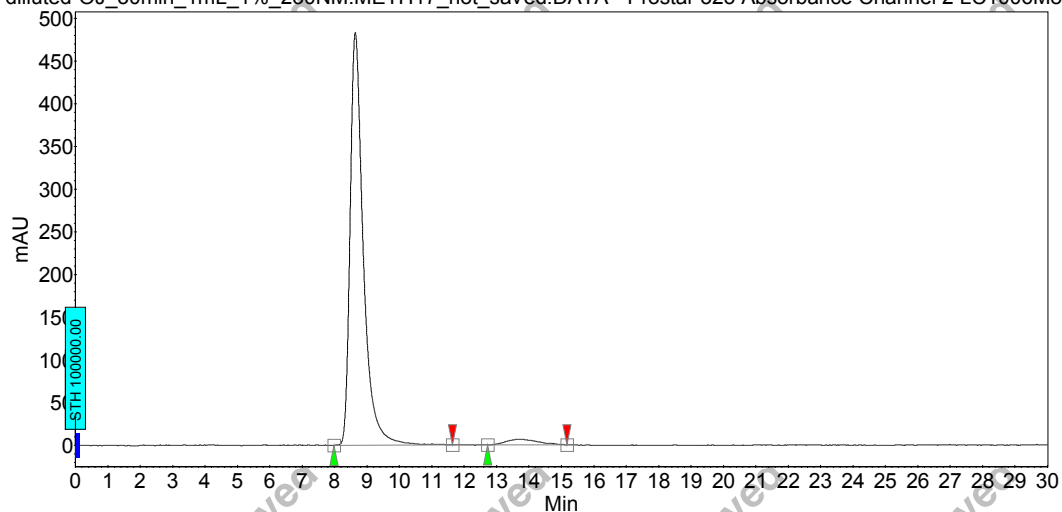


Peak results :

| Index | Name | Time [Min] | Quantity [% Area] | Height [mAU] | Area [mAU.Min] | Area % [%] |
|-------|---------|------------|-------------------|--------------|----------------|------------|
| 1 | UNKNOWN | 8.35 | 98.01 | 1959.3 | 636.1 | 98.005 |
| 2 | UNKNOWN | 13.48 | 1.99 | 14.2 | 12.9 | 1.995 |
| Total | | | 100.00 | 1973.5 | 649.0 | 100.000 |

0.001 mol% at 60 °C

pcl-100-2-dilluted-OJ_30min_1mL_1%_230NM.METH17_not_saved.DATA - Prostar 325 Absorbance Channel 2 LC1006M831

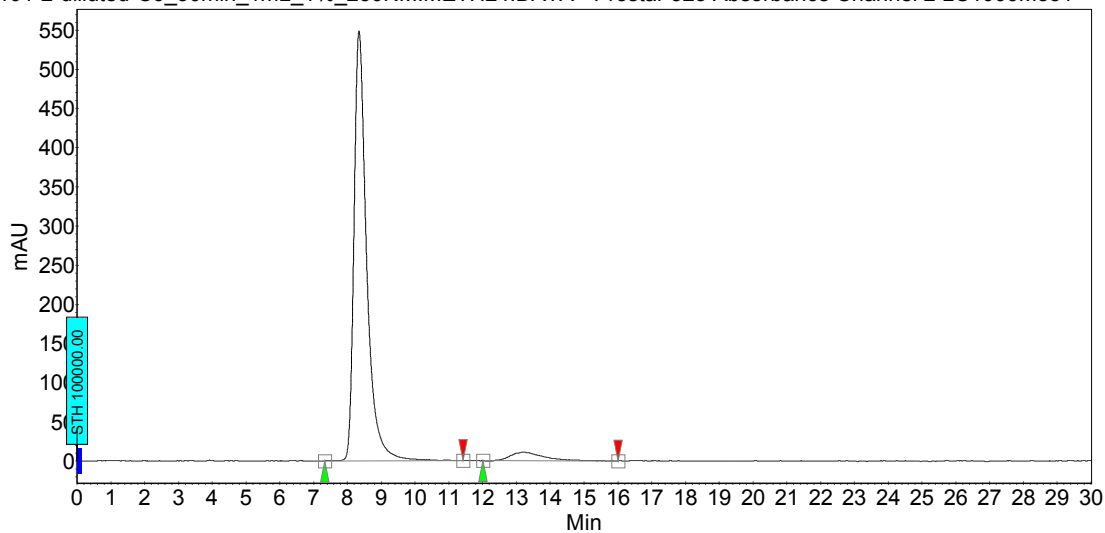


Peak results :

| Index | Name | Time [Min] | Quantity [% Area] | Height [mAU] | Area [mAU.Min] | Area % [%] |
|-------|---------|------------|-------------------|--------------|----------------|------------|
| 1 | UNKNOWN | 8.64 | 96.89 | 483.1 | 227.3 | 96.892 |
| 2 | UNKNOWN | 13.75 | 3.11 | 6.6 | 7.3 | 3.108 |
| Total | | | 100.00 | 489.7 | 234.6 | 100.000 |

0.00025 mol% at 60 °C

pcl-101-2-dilluted-OJ_30min_1mL_1%_230NM.METH24.DATA - Prostar 325 Absorbance Channel 2 LC1006M831

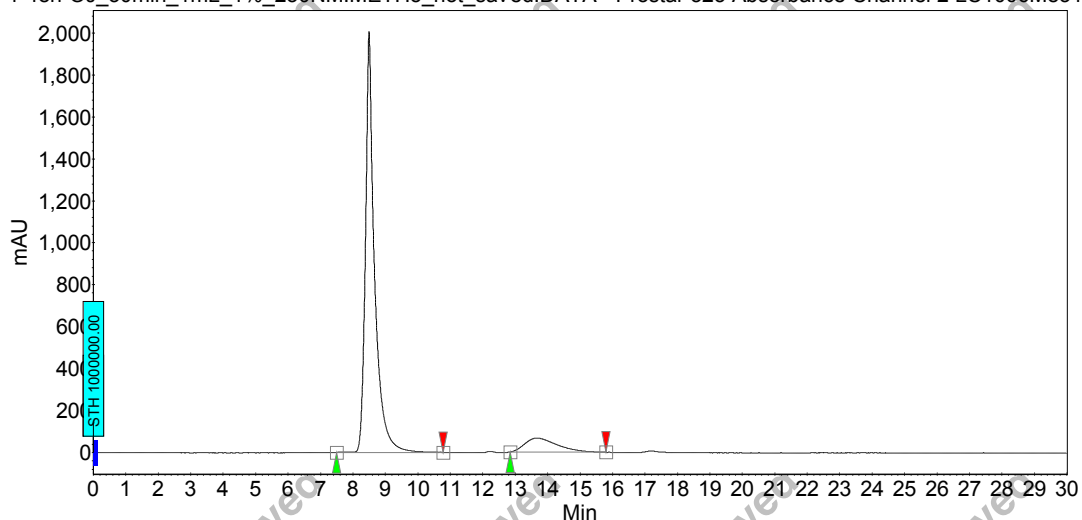


Peak results :

| Index | Name | Time [Min] | Quantity [% Area] | Height [mAU] | Area [mAU.Min] | Area % [%] |
|-------|---------|------------|-------------------|--------------|----------------|------------|
| 1 | UNKNOWN | 8.34 | 95.09 | 548.9 | 237.8 | 95.091 |
| 2 | UNKNOWN | 13.22 | 4.91 | 10.8 | 12.3 | 4.909 |
| Total | | | 100.00 | 559.6 | 250.1 | 100.000 |

Attempting 1M TON with Rh₂(S-p-Br-TPCP)₄, 70 °C, 2.32 equiv. styrene

pcl-104-1-48h-OJ_30min_1mL_1%_230NM.METH5_not_saved.DATA - Prostar 325 Absorbance Channel 2 LC1006M831

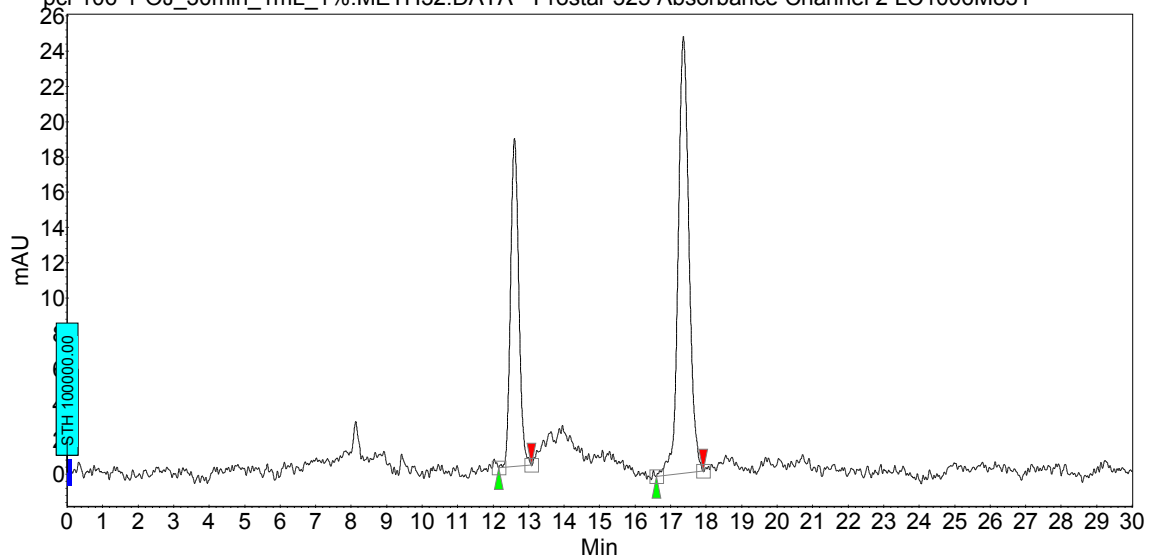


Peak results :

| Index | Name | Time [Min] | Quantity [% Area] | Height [mAU] | Area [mAU.Min] | Area % [%] |
|-------|---------|------------|-------------------|--------------|----------------|------------|
| 1 | UNKNOWN | 8.50 | 89.38 | 2005.2 | 649.0 | 89.375 |
| 2 | UNKNOWN | 13.65 | 10.62 | 66.4 | 77.2 | 10.625 |
| Total | | | 100.00 | 2071.6 | 726.2 | 100.000 |

Attempting 1M TON with Rh₂(R-TPPTTL)₄

pcl-106-1-OJ_30min_1mL_1%.METH32.DATA - Prostar 325 Absorbance Channel 2 LC1006M831

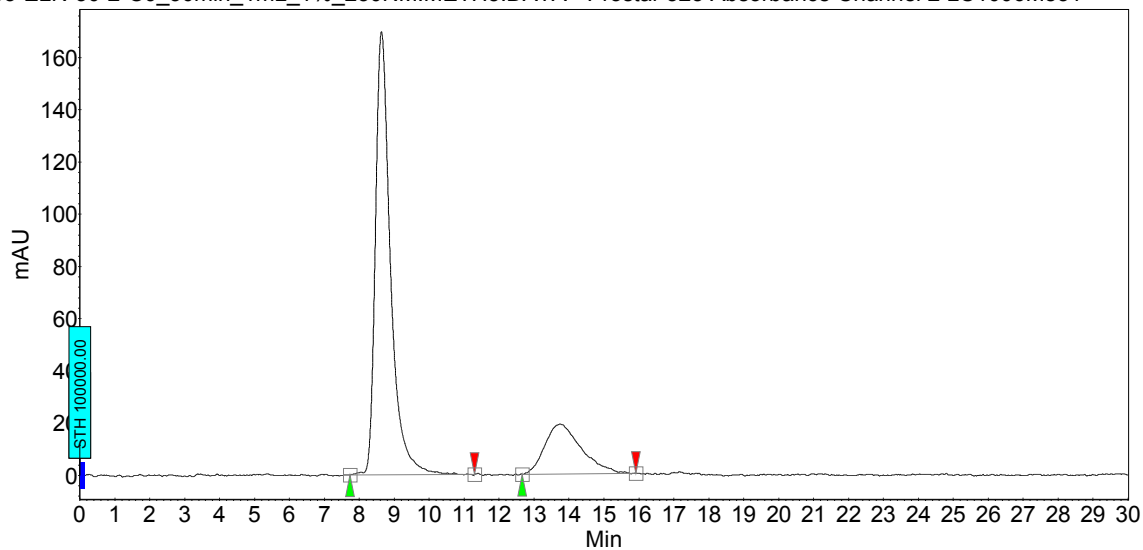


Peak results :

| Index | Name | Time [Min] | Quantity [% Area] | Height [mAU] | Area [mAU.Min] | Area % [%] |
|-------|---------|------------|-------------------|--------------|----------------|------------|
| 1 | UNKNOWN | 12.60 | 36.39 | 18.6 | 5.0 | 36.394 |
| 2 | UNKNOWN | 17.36 | 63.61 | 24.8 | 8.8 | 63.606 |
| Total | | | 100.00 | 43.4 | 13.8 | 100.000 |

Attempting 1M TON with $\text{Rh}_2(\text{S-TPPTTL})_4$

Bo-ELN-30-2-OJ_30min_1mL_1%_230NM.METH5.DATA - Prostar 325 Absorbance Channel 2 LC1006M831

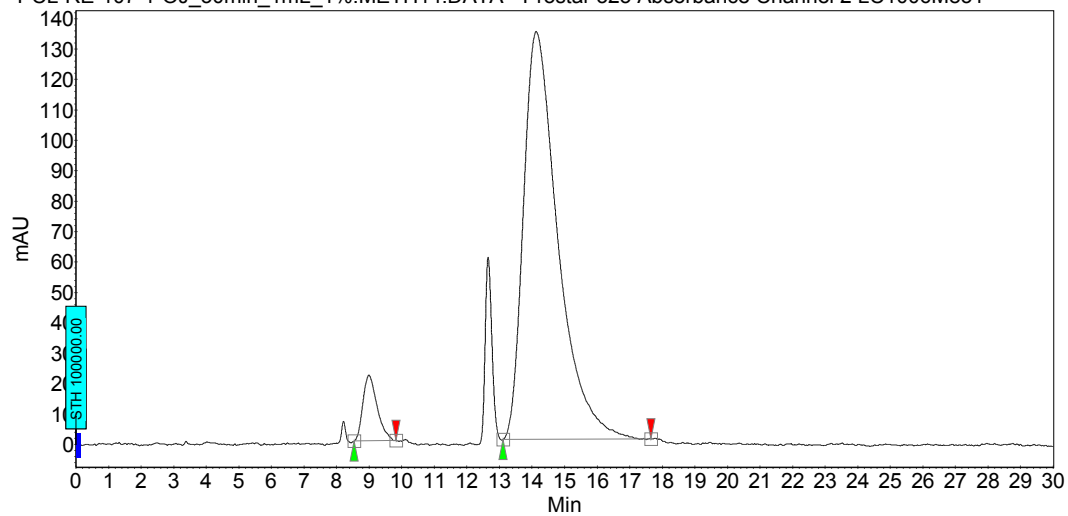


Peak results :

| Index | Name | Time [Min] | Quantity [% Area] | Height [mAU] | Area [mAU.Min] | Area % [%] |
|-------|---------|------------|-------------------|--------------|----------------|------------|
| 2 | UNKNOWN | 8.63 | 78.71 | 169.6 | 85.2 | 78.710 |
| 1 | UNKNOWN | 13.75 | 21.29 | 19.2 | 23.0 | 21.290 |
| Total | | | 100.00 | 188.8 | 108.2 | 100.000 |

Attempting 1M TON with $\text{Rh}_2((1\text{S},2\text{S})\text{-p-Br-2-TMS-DPCP})_4$

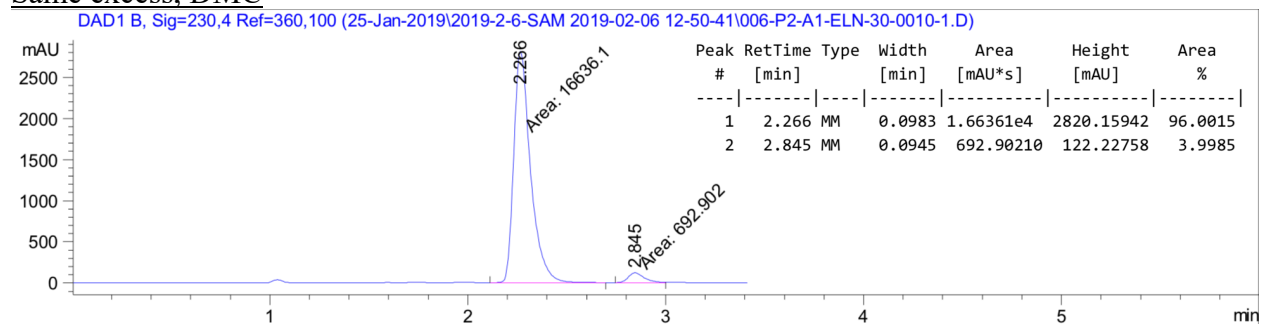
PCL-RE-107-1-OJ_30min_1mL_1%.METH14.DATA - Prostar 325 Absorbance Channel 2 LC1006M831



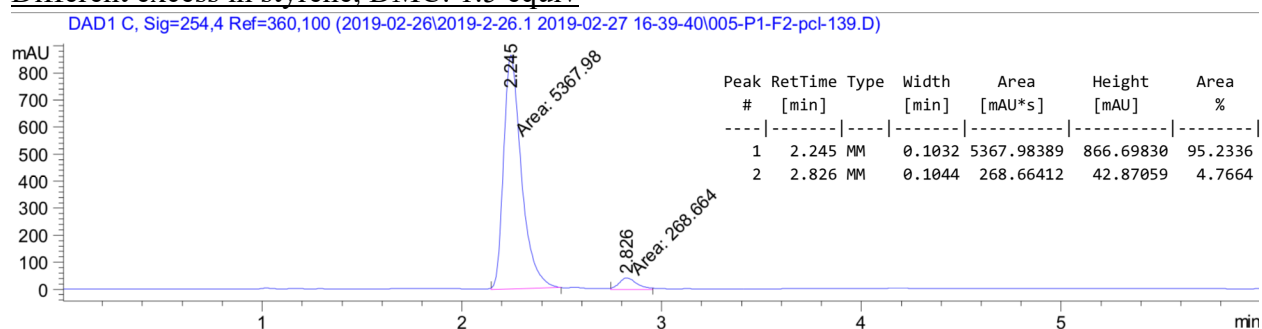
Peak results :

| Index | Name | Time [Min] | Quantity [% Area] | Height [mAU] | Area [mAU.Min] | Area % [%] |
|-------|---------|------------|-------------------|--------------|----------------|------------|
| 1 | UNKNOWN | 8.99 | 6.24 | 21.6 | 10.9 | 6.235 |
| 2 | UNKNOWN | 14.12 | 93.76 | 134.0 | 163.8 | 93.765 |
| Total | | | 100.00 | 155.7 | 174.7 | 100.000 |

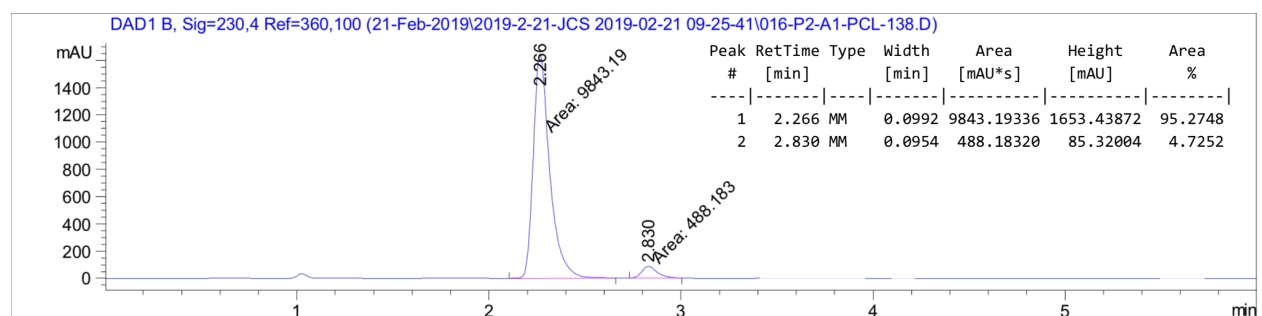
Same excess, DMC



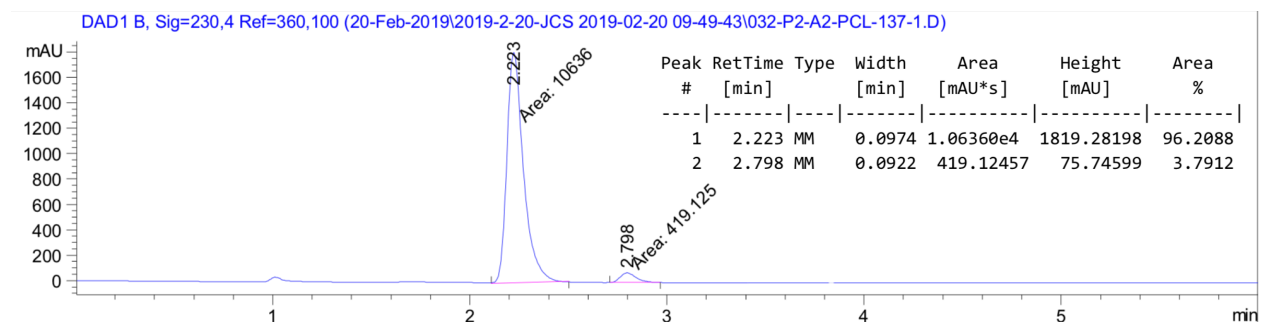
Different excess in styrene, DMC: 1.5 equiv



Different excess in styrene, DMC: 4.64 equiv.



Different excess in diazo, DMC: 0.5g diazo



References

- [1] Davies, H. M. L.; Bruzinski, P. R.; Lake, D. H.; Kong, N.; Fall, M. J. *J. Am. Chem. Soc.* **1996**, *118*, 6897.
- [2] Qin, C.; Boyarskikh, V.; Hansen, J. H.; Hardcastle, K. I.; Musaev, D. G.; Davies, H. M. L. *J. Am. Chem. Soc.* **2011**, *133*, 19198–19204.
- [3] Qin, C. M.; Davies, H. M. L. *J. Am. Chem. Soc.* **2014**, *136*, 9792.
- [4] Reddy, R. P.; Davies, H. M. L. *Org. Lett.* **2006**, *8*, 5013.
- [5] Negretti, S.; Cohen, C. M.; Chang, J. J.; Guptill, D. M.; Davies, H. M. L. *Org. Lett.* **2013**, *15*, 6136.
- [6] Level, H.; Marcoux, J. F.; Molinaro, C.; Charette, A. B. *Chem. Rev.* **2003**, *103*, 977.
- [7] Talele, T. T. *J. Med. Chem.* **2016**, *59*, 19, 8712-8756.
- [8] Nowlan, D. T.; Gregg, T. M.; Davies, H. M. L.; Singleton, D. A. *J. Am. Chem. Soc.* **2003**, *125*, 51, 15902-15911.
- [9] Hansen, J.; Autschbach, J.; Davies, H. M. L. *J. Org. Chem.* **2009**, *74*, 6555–6563.
- [10] Davies, H. M. L.; Morton, D. *Chem. Soc. Rev.* **2011**, *40*, 1857.
- [11] Pelphrey, P. I.; Hansen, J.; Davies, H. M. L. *Chem. Sci.* **2010**, *1*, 254.
- [12] Blackmond, D. G. *Angew. Chem. Int. Ed.* **2005**, *44*, 4302-4320.
- [13] Fullilove, F. A. *In situ* Kinetic Studies of Reactions Involving Dirhodium (II) Donor/Acceptor Carbenes. Ph. D. Thesis, Emory University, 2014.
- [14] Burés, J. *Angew. Chem. Int. Ed.* **2016**, *55*, 2028-2031.
- [15] Tundo, P.; Aricò, F.; Rosamilia, A. E.; Grego, S.; Rossi, L. *NATO Sci. Peace. Sec. C.* **2008**, 213-232.
- [16] Guptill, D. M.; Davies, H. M. L. *J. Am. Chem. Soc.* **2014**, *136*, 51, 17718-17721.